Nanoneedle-based Sensing in Biological Systems

Ciro Chiappini*

Centre for Craniofacial and Regenerative Biology, King's College London, SE1 9RT, London, United Kingdom. ciro.chiappini@kcl.ac.uk

Abstract

Nanoneedles are high aspect ratio nanostructures with a unique biointerface. Thanks to their peculiar yet poorly understood interaction with cells, they very effectively sense intracellular conditions, typically with lower toxicity and perturbation than traditionally available probes. Through long-term, reversible interfacing with cells, nanoneedles can monitor biological functions over the course of several days. Their nanoscale dimension and the assembly into large scale, ordered, dense arrays enable monitoring the functions of large cell populations, to provide functional maps with sub-micron spatial resolution. Intracellularly, they sense electrical activity of complex excitable networks, as well as concentration, function and interaction of biomolecules *in situ*, while extracellularly they can measure the forces exerted by cells with piconewton detection limits, or efficiently sort rare cells based on their membrane receptors. Nanoneedles can investigate the function of many biological systems, ranging from cells, to biological fluids, to tissues and living organisms. This review examines the devices, strategies and workflows developed to use nanoneedles for sensing in biological systems.

Keywords

Nanoneedles, nanowires, biointerface, intracellular sensing, review, biomarkers, label-free, minimally invasive.

Nanoneedles are rapidly emerging as a tool to interact with the intracellular environment of large number of cells simultaneously, with limited perturbation of their physiological processes. This interaction provides characteristics advantages for minimally invasive cell and molecular biology investigations, as well as to progress biomedical translation of regenerative and precision medicine approaches. A quick string of several successful proofs of principles have established nanoneedles' potential to efficiently deliver impermeant molecules[1,2] and nanoparticles[3] directly to the cell cytosol, and to sense the intracellular milieu[4-6] across biological systems ranging from cells in culture[7] to living organisms[8]. Nanoneedles can be broadly defined as nanomaterials whose high aspect ratio enables their biological interaction; this definition encompasses a broad range of classically defined nanomaterials, which cater for different biointerfacing needs and applications (Figure 1).

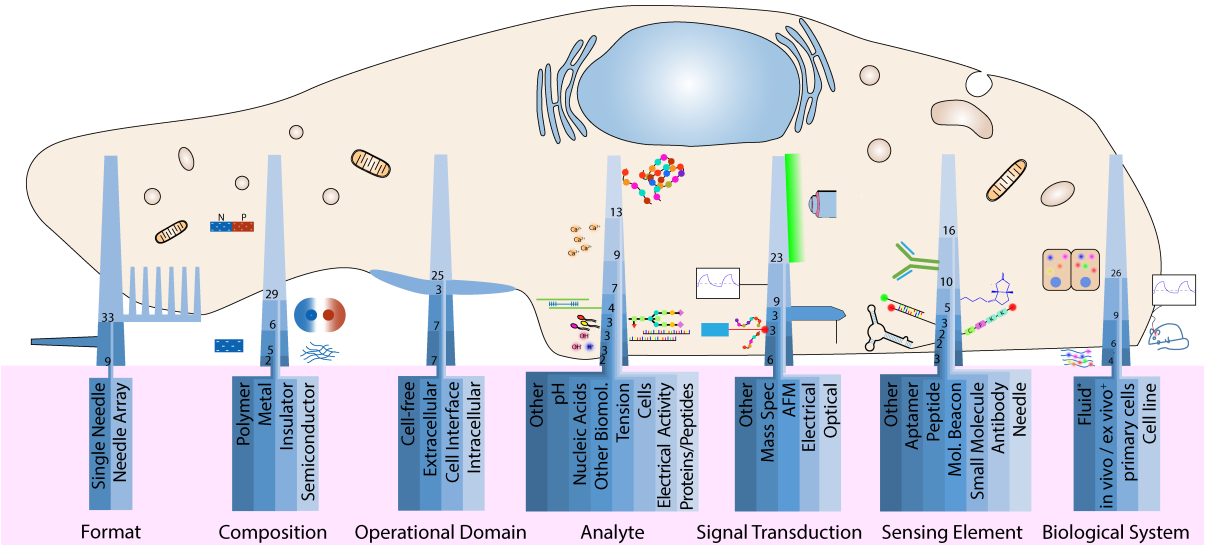

Figure 1 Overview of the nanoneedle devices and strategies used for sensing in biological systems. Each nanoneedle is a stacked bar of a bar graph. The legend below each nanoneedle is color-coded and connects to the associated bar. The height of each bar represents the fraction of reviewed papers with that characteristic. The number in each bar is the number of reviewed publications with that characteristic. Numbers for each bar do not sum to the same total as publications can contribute to more than one bar in a given stack. *"Fluid" excludes biological fluids, + "in vivo/ex vivo" includes biological fluids. The overview is compiled from all the publications reviewed herein that include sensing work.

Nanoneedles belong to two main classes; they are either single needles that are externally manipulated to come in contact with cells and tissues[9], or arrays of vertical high aspect ratio nanostructures supported on a substrate[10]. Single nanoneedles are most commonly nanowires operated either through an AFM[9] or through micromanipulators[11]. Nanoneedle arrays, instead, encompass a wide variety of nanostructures including nanowires[1], nanopillars[12], porous nanocones[2], nanotubes[13] and nanostraws[14]. Each structure has different enabling properties that befit specific sensing needs. The disordered structure of nanowires enhances the interaction with multiple sites across the cell, with benefits for the specific capture of rare cells[15]. The defined geometry of nanopillars enables tailoring their

mechanical properties to modulate their interaction with cells[16] and to accurately sense forces applied by cells[17]. The geometry of nanocones improves their stability over cylindrical structures, and their porosity improves the available surface for interaction with analytes while making them biodegradable, a crucial property for *in vivo* applications[2,18]. Nanostraws are a class of nanotubes open on both ends, with one end connected to a fluid reservoir. In this way, nanostraws act as an open physical conduit between intracellular and extracellular fluids, enabling their sustained and controlled exchange[14,19].

Due to the broad variety of nanostructures, there are many fabrication strategies to obtain nanoneedles; these include the broadly established vapor-liquid-solid growth of semiconductor nanowires and nanotubes, deposition techniques for metal nanostructures, dry etching for nanopillars, metal assisted electrochemical etching for nanowires and nanocones, focused ion beam milling for a large share of the single nanoneedles, combinations of deposition and etching with sacrificial templates for nanostraws, and replica molding for polymeric structures. When looking at nanoneedles used for sensing, semiconductors, and within them silicon, take the lion's share of the materials used, likely due to the advanced manufacturing techniques established by the microfabrication industry coupled with their favorable and tailorable electrical and photonic characteristics. Yet the properties of metals, dielectrics and even polymers are crucial for specific applications. The conductivity and chemical inertness of noble metals find its application for electrical sensing[6], and their plasmon resonance for enhanced Raman spectroscopy[13]. The optical transparency of dielectrics enables easier, live visualization of the interaction with cells[16], and provides waveguides[20] and optical apertures[12] with subwavelength characteristic dimensions. The motility of soft polymer nanoneedles finds advantages for enhanced specific recognition of cells[21].

Nanoneedles serve primarily to sense the intracellular environment and the interface between cells and their surrounding, since these are the applications where their high aspect ratio and minimal invasiveness provide the largest advantages. Yet the high surface area available for selective capture/interaction[15,22], and the out-of-substrate-plane defined location of nanoneedle arrays[23] provide advantages for sensing within biological fluids and in the extracellular environment[22,24]. Biomolecules and their interactions are the main analyte of nanoneedle-based sensing, thanks to the unique potential to probe them in their unperturbed intracellular conditions. Among these proteins, peptides and their metabolic interactions have been the most investigated[18,25]. Nanoneedles can also sense nucleic acids[26], as well as lipids[13] and carbohydrates[27]. Electrical activity is the other major sensing application for nanoneedles[28], largely underrepresented in this review, given the vastness of the field and existing high quality, recent reviews on the subject [24,28,29]. This review tries to focus on few key applications where the nanoscale, high aspect ratio characteristics are enabling for the nature of electrical sensing, and on significant milestones for translational advancement.

Nanoneedles can detect and sort circulating cancer cells within biological fluids[30], since their enhanced interaction enables more effective capture. Other notable efforts are those related to measuring intracellular conditions, such as pH[3], which can provide an overall indication of cell metabolism, and the measurement of cell tension through the force they exert [17]. The signal from this wide variety of targets requires different transduction mechanisms. Electrical transduction senses electrical signaling, while optical transduction senses the vast majority the other signals. Peptides and proteins are also sensed electrically[22], by mass spectrometry[7] and by AFM force-displacement curves[31]. A broad range of sensing elements are necessary to

address this wide variety of targets. The needle structure itself is sufficient and often enabling for electrical sensing[32], photonic/Raman signals[33] and the detection of cell forces[17], while specific ligand-receptor interaction enables recognition of biomolecules and their interaction[34]. Environmentally-sensitive fluorophores or Raman probes mediate pH sensing[35]. Equipped with this toolset, nanoneedles can sense biological systems across a wide range of complexities: from biological fluids[22], to established cells lines[4], more susceptible primary and stem-derived cells[36], as well as complex tissues *in vivo*[8] and *ex vivo*[2].

The biointerface

The interface between nanoneedles and biological systems is highly peculiar. Due to the high aspect ratio and the characteristic nanoscale dimensions, nanoneedles intimately contact large traits of the cell membrane, strongly interacting with it and with the intracellular milieu[16,37,38] (Figure 2).

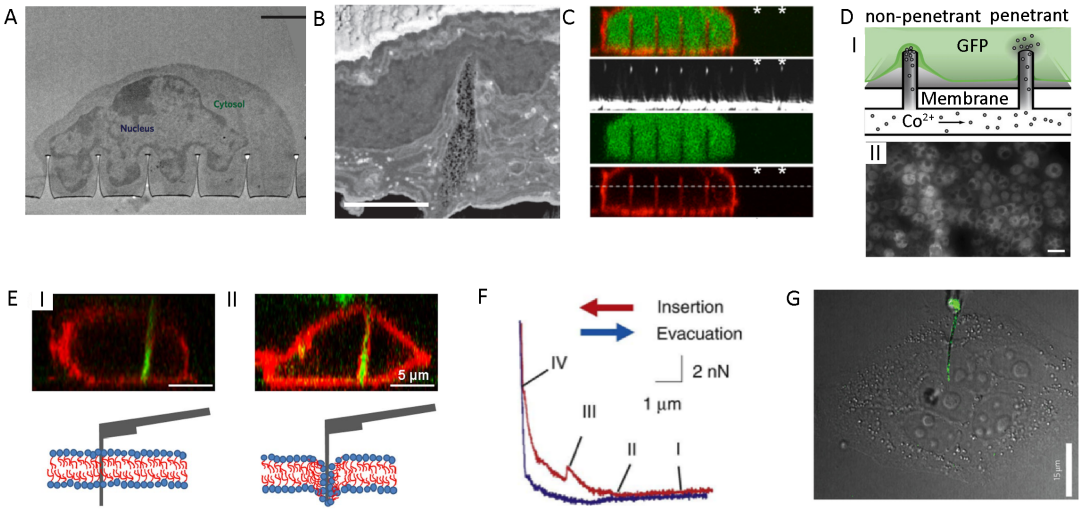

Figure 2 The cell-nanoneedle interface. *Due to their nanoscale and high aspect ratio, nanoneedles interact strongly with the cell membrane. This interaction underpins their intracellular delivery and sensing. (A) A silicon dioxide nanopillars array does not insert within the cell cytosol, but deforms the plasma and nuclear membranes. Scale bar 2 µm. Reprinted by permission from Macmillan Publishers Ltd: Nat. Nanotechnol. [16], copyright (2015). (B) Porous silicon nanoneedle arrays interface extensively with the cell cytosol and deform the nuclear membrane. Scale bar 1 µm. Reprinted by permission from Macmillan Publishers Ltd: Nat. Mater. [2], copyright (2015). (C) InAs nanoneedles arrays do not insert within the cell cytosol and strongly deform the plasma membrane (Red). Republished with permission of IOP Publishing, from [39] copyright 2012. (D) Approximately 7% of nanostraws can deliver the membrane-impermeant ion Co^{2+} to the cell cytosol, where it quenches GFP fluorescence. (I)Schematic of the delivery mechanism, (II) GFP quenching spots observed by optical microscopy. Scale bar 20 µm. Reprinted by permission from Macmillan Publishers Ltd: Nat. Comm. [40], copyright (2014). (E) Cytosolic insertion of AFM operated nanoneedles depend on apparent membrane fluidity, which can be determined by insertion speed, temperature and cell conditions. (I) AFM nanoneedle (green) successfully inserted is not surrounded by plasma membrane (Red), while (II) unsuccessfully inserted one is. Scale bars 5 µm. Reproduced under creative commons license from[41]. (F) Cytosolic insertion of AFM nanoneedles is detected by a sudden drop (III) the force-displacement curve. Reprinted from [42], Copyright (2008), with permission from Elsevier. (G) Micromanipulator operated*

nanoneedles can insert within the cell cytosol. Scale bar 15 µm. Reproduced with permission from Reprinted by permission from Macmillan Publishers Ltd: Nat. Nanotechnol. [43]*, copyright (2010).*

It is this unique interaction, whose details are still largely unexplored, that enables their superior ability to investigate the intracellular space. In order to grasp the mechanisms through which nanoneedles sense the intracellular milieu it is thus fundamental to recapitulate our current understanding of their interface with biological systems. The nature of the cell-nanoneedle interface varies strongly with the details of the system, with significant impact on the efficiency of nanoneedles to probe the intracellular environment (Table 1). The length, diameter, density and in general the geometry of the needles, their composition, as well as the type of cell and the mechanism of interfacing influence the interaction, ultimately resulting in different mechanisms of access to intracellular information, not all of which are yet clarified. Interfacing occurs either by allowing the cells to adhere and spread over nanoneedles or by forcefully applying the nanoneedles over cells or tissues[3]. In the first instance, cell suspensions are simply dispensed over the nanoneedles, following which the cells are the only active player that determine the evolution of the interfacing with the substrate. The details of the interface achieved with this strategy are still largely unexplored. Cell lines as well as primary cells known to be particularly susceptible to membrane integrity, such as neurons and cardiomyocytes retain high viability when seeded over arrays of nanowires[44], nanopillars[32], nanocones[6] and nanotubes[45]. Transmission electron microscopy of nanopillars[38] and confocal microscopy of nanowires[39] indicate that there is close contact between nanoneedles and the cell membrane without them inserting in the intracellular space (Figure 2A-C). In most cases, recording intracellular action potentials require prior electroporation of the cells, and is lost within a few minutes, further supporting the preserved integrity of the plasma membrane and the extracellular nature of the nanoneedle interface[28,32,36]. Conflicting confocal microscopy evidence from nanowires does not show the presence of cell membrane enveloping the nanoneedles[1]. Nonetheless the absence of fluorescent signal around the vertical walls of nanoneedles may not indicate the absence of the cell membrane, and simply be a consequence of the observed suppression of fluorescent signal along the nanoneedles stem in contrast to its enhancement at the tip[46,47].

Yet a wide range of cell-impermeant payloads, including ions[40], peptides[18], proteins[1,2], nucleic acids[1,2], polysaccharides[27] and nanoparticles[48] are efficiently delivered from the nanoneedles to the cytosol of cells, indicating a direct communication between the cell's exterior and its interior through the nanoneedles. The geometry of the nanoneedles and the type of cells was shown to influence delivery efficiency[49]. In particular, using nanostraws (Al_2O_3) to deliver the membrane-impermeant Co^{2+} ion allows studying the frequency with which nanoneedles can access the cytosol[40,50] (Figure 2D). In this setup, nanostraws delivering Co^{2+} ions intracellularly, locally quench the fluorescence of cells expressing GFP throughout the cytosol. Counting the fraction of GFP-quenching spots shows that 7% of nanostraws have direct access to the cytosol. Further experiments with the same system show that the cell membrane and the underlying cytoskeletal network act as synergistic barriers to prevent cytosolic access[51]. Using a combination of dimethyl sulfoxide to permeabilize the cell membrane and Latrinculin A to destabilize cytoskeletal assembly, shows that only the combined action of the two agents significantly increases the rate of nanostraws accessing the cytosol from 8% to 13%. This set of studies is accompanied by a theoretical model that proposes how nanoneedles could insert within cells due to the local forces generated by the traction of cells at the tip of the needles.[52] The forces a cell generates on a nanoneedle according to this model are in excess of those sufficient for the penetration of a single AFM-operated needle. Nonetheless the AFM

literature indicates that rapid nanoneedle movement is necessary for insertion, regardless of the the magnitude of the applied force[41,53]. The evidence available at this stage suggest that seeding cells over nanoneedles yields an intimate contact with the membrane that facilitates interaction with the intracellular space, but nanoneedle arrays do not necessarily insert within the cell.

Several strategies have been developed to forcefully interface the nanoneedles with cells. Single needles are usually either the tip of an AFM probe or are mounted at the end of a probe operated with a micromanipulator. These needles routinely interface with cells using linear actuators that move them against the cell membrane. Several publications with AFM-operated nanoneedles provide the most convincing evidence that this interfacing strategy can insert single nanoneedles within the cytosol with high efficiency. By analysing the force-displacement curve during the approach to cells of the AFM-operated nanoneedles (Si) it is possible to identify sudden drops in force attributable to insertion[9,53] (Figure 2E-F) . The attribution of the drops is validated by confocal imaging of inserted and non-inserted nanoneedles[41,42,54], and by intracellular sensing with inserted nanoneedles[4,26]. This forceful insertion preserves cell viability, provided that the diameter of the nanoneedle is below the cutoff value of 400nm[55]. Yet, insertion efficiency depends crucially on several parameters. While increasing the force applied to the needle has little impact on insertion, Increasing the speed of interfacing correlates with its yield[41]. Insertion speeds of 3–10 µm/s are necessary to achieve high insertion yields. The stiffness of the cell, as mediated by cytoskeletal tension, is also crucial for insertion. Oppositely from what observed for nanoneedle insertion in the absence of applied forces, in this case cytoskeletal tension is a necessary prerequisite for efficient insertion. Membrane fluidity also plays a significant role in insertion efficacy, with better efficiencies achievable by reducing it[41]. Modulating the affinity of nanoneedles' tip by inserting hydrophobic molecules that promote fusion with the cell membrane also enhances insertion efficiency[56,57]. There is direct evidence that nanoneedles operated by micromanipulators can gain access to the intracellular space by forcing their way through the cell membrane, but unlike AFM nanoneedles there is no detailed study of the parameters conducive to their insertion[20,33,43] (Figure 2G). Decorating these nanoneedles with phospholipids[45], hydrophobic silanes[58] or cell penetrating peptides[59] enables intracellular insertion without applied forces[11].

Arrays of nanoneedles also interface with cells through force application. These strategies are are varied, and include hypergravity through centrifugation[60], manual application of forces[18], linear actuation[61], and high-frequency oscillating piezoelectric movements for rapid, repeated interfacing[61]. All these strategies improve the ability of nanoneedles to sense from and delivery within the cell, but, similarly to what observed for cell seeding on nanoneedle arrays, there is no direct evidence that any of them can insert nanoneedles within cells. Suspensions of cells can be centrifuged over nanoneedle arrays[62], or vice versa nanoneedles can be centrifuged over cells adherent to a substrate[2]. Hypergravity values ranging from 12.8g to 35.5g yield improve cell interfacing from 5% to 80%, as measured through delivery efficiency, while preserving viability[60]. A custom-design high speed linear actuator for nanoneedle arrays enables controlled interfacing[61]. The actuator tilts the array so that it is parallel to the cell culture substrate in order to maximize the number of interacting cells, and then lowers it at a defined speed until it makes contact. Further equipped with a piezoelectric crystal, the actuator can oscillate the nanoneedles when in contact with cells. This approach

improves cell interfacing, as measured by the efficiency of gene expression following plasmid delivery, surprisingly with minimal impact on cell viability.

The many geometries, compositions and mechanisms of interfacing for nanoneedles, complicate a systematic assessment of cytotoxicity that can derive clear guidelines. In general, the vast majority of the systems available have all reached a degree of optimization such that they present minimal toxicity and invasiveness for the biological systems they have been tested with. *In vitro*, AFM operated nanoneedles (Si) display a threshold for a sharp increase in toxicity at 400 nm in diameter[60]. Despite cytotoxicity is not reported in all instances, several strategies for forceful application of nanoneedles, including hypergravity[60], mechanical actuation[43], and piezoelectric oscillation [61] retain cell viability comparable to controls. Similarly, nanostraws (Al_2O_3) are not toxic to primary cells, despite being able to extract up to 10% of intracellular reporter proteins[19]. Equally, with optimized geometries, seeding cells over nanoneedles does not induce toxicity, including primary cells of known sensitivity to membrane integrity, such as primary neurons[6] and cardiomyocytes[36]. Yet, increasing nanoneedle length beyond that allowing for cells to interact with the underlying substrate increases cytotoxicity[63]. *In vivo*, nanoneedles do not alter the structure of the tissue they interface with either in the short or in the long term[2]. Further the target tissues do not present signs of acute or chronic immune response [2].

Interfacing strategy	**Force applied?**	**Tunable Parameters**	**Interfacing efficiency* (%)**	**Key Ref#**
Seeding	N	Cell density	>90	[2]
Hypergravity	Y	Acceleration Duration	~80	[60]
AFM	Y	Force Speed	70	[42]
Piezo oscillation	Y	Distance Duration	42	[61]
Micromanipulation	Y/N	Position	>90	[43]

*Table 1 Cell-nanoneedle interfacing strategies and their efficiency. *interfacing efficiency is determined from the most favourably reported intracellular interaction observed for the given strategy. #Key reference is the publication from which the interfacing efficiency has been derived.*

Detecting cells

The enhanced interaction of nanoneedles with the cell membrane increases the potential to detect and capture cells by the moieties they present at the cell surface. Using this principle, nanoneedle arrays can recognize circulating tumor cells (CTCs). CTCs can be present at ultralow concentration in the blood of cancer patients (Table 2). Their presence, their number and their phenotype can provide critical diagnostic and prognostic information for clinicians to use for personalized treatments. Due to the rarity and heterogeneity of these cells it is essential to develop strategies for their efficient and selective capture that rapidly and robustly screen milliliter quantities of blood. The captured cells should then be preserved viable and made readily available for downstream analysis.

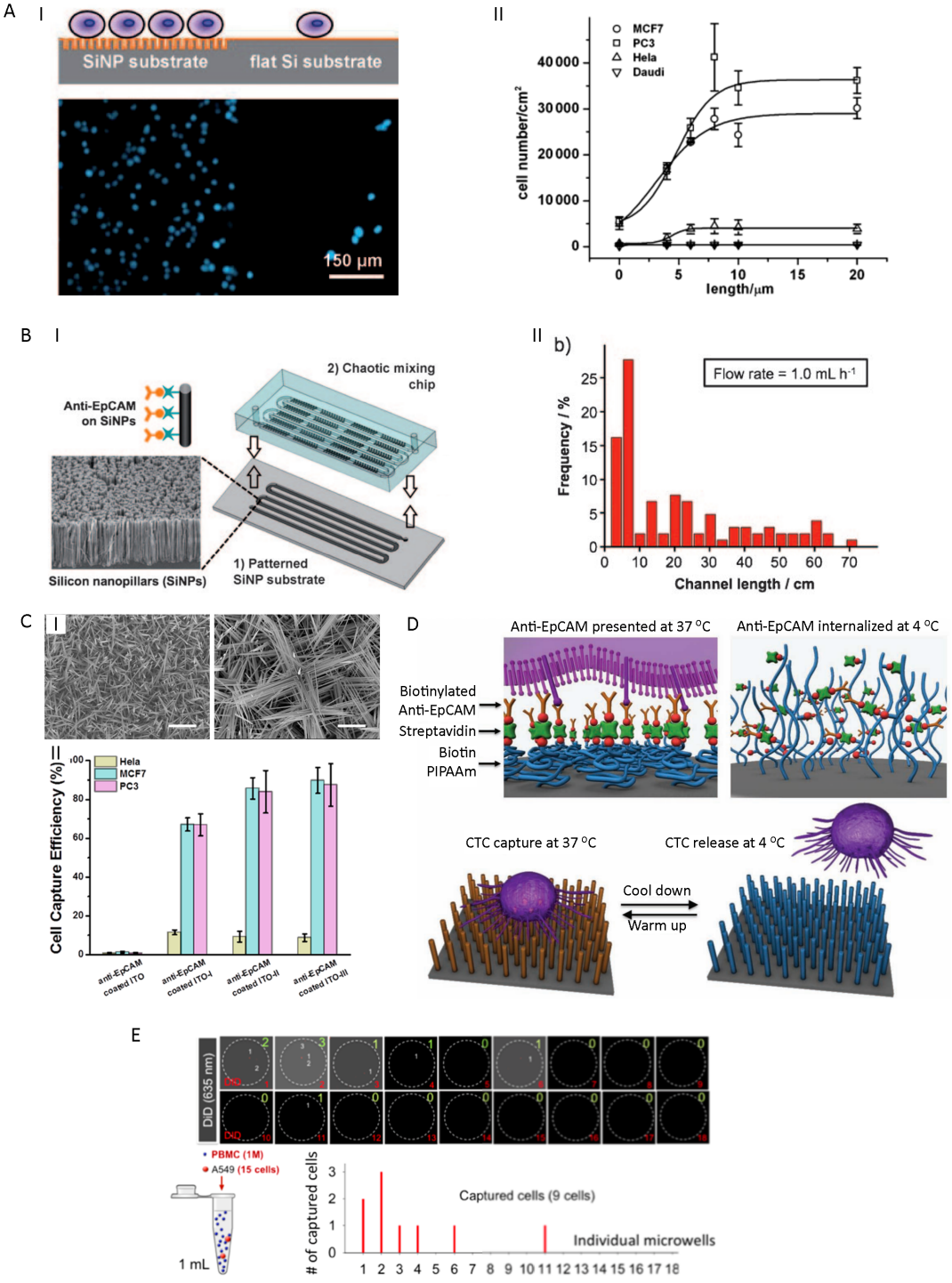

Figure 3 Detecting circulating tumour cells. Nanoneedle arrays enhance specific capture (EpCAM-antibody mediated) and detection of circulating cancer cells thanks to their geometry conducive to more effective interaction with the cell membrane. (A) A silicon nanowire array (I) captures EpCAM positive cells more efficiently than a neighboring flat silicon substrate. (II) The capture efficiency is correlated with the length of the nanowires, with a plateau at 6µm; non-specific capture of EpCAM negative cells is significantly lower than specific capture. Reproduced with permission from[64]. Copyright © 2009 WILEY-VCH Verlag GmbH & Co. KGaA, Weinheim. (B) Integrating the silicon nanowire array (I) within a microfluidic chaotic mixing chip enhances capture efficiency. (II) The microfluidic flow rate affects capture efficiency and the distribution of captured cells along the channel. Reproduced with permission from[54]. Copyright © 2011 WILEY-VCH Verlag GmbH & Co. KGaA,

Weinheim. (C) Hierarchical ITO nanowires for circulating cancer cell capture. (I) SEM showing first-generation (left) and second generation (right) ITO nanowires. (II) Increasing generations of the ITO nanowires improve the capture efficiency, with no effect on non-specific capture. Reprinted with permission from [15]. Copyright 2016 American Chemical Society. (D) Schematic depiction of the capture and release of circulating cancer cells from silicon nanowire arrays functionalized with thermoresponsive pNIPAMM. Cells are efficiently captured through EpCAM recognition at 37 ^{o}C and released from the substrate at 4 ^{o}C, due to the changes in conformation of the PNIPAm. Reproduced with permission from[30]. Copyright © 2013 WILEY-VCH Verlag GmbH & Co. KGaA, Weinheim. (E) Direct analysis on-chip of captured circulating tumor cells. Laser scanning cytometry acquires high content images of nanoneedle arrays and can detect nine out of fifteen EpCAM positive cells spiked within 1 million PBMC cells. Reprinted with permission from [65]. Copyright 2012 American Chemical Society.

Nanoneedles (Si) decorated with anti-EpCAM antibody capture EpCAM positive cancer cells from solution with an efficiency between 45-65% improving upon the 4-14% achievable with anti-EpCAM decorated flat surfaces[64] (Figure 3 A). Prolonging incubation of the cells on the needles, up to 45 minutes, improves capture efficiency. The capture of EpCAM negative cells also depends on incubation time but remains significantly lower than positive cells. The length of the nanowires influences capture efficiency, requiring nanowires of 6 µm or longer for optimal capture efficiency. The nanowires can capture EpCAM positive cells spiked within blood at densities ranging from 1000 down to 5 cells mL^{-1}. At the lowest cell concentration, the capture rate is around 50%. Importantly, cell viability with this approach reaches 91%, which can enable downstream analysis. Integrating this system in a microfluidic device further improves its efficiency[54] (Figure 3B). The device is assembled by overlaying an 88 cm long serpentine PDMS microchannel over a nanowire substrate. Chevrons texturing the PDMS channel promote chaotic microfluidic mixing, with the aim to enhance the interaction between cells and the nanowire substrate. With this strategy the capture of EpCAM positive cells from solution can reach over 95% efficiency, provided that the flow rate is maintained below 2 ml h^{-1}. For higher flow rates capture efficiency rapidly drops, to below 30% at 7 ml h^{-1}. The location of cell capture also changes with flow rate. At 1 ml h^{-1} cells are largely captured within the first quarter of the channel, but with increasing rates they rapidly spread out to the entire channel length. The analysis of 30 blood samples of prostate cancer patients with this system shows that it could capture CTCs in greater numbers than the CellSearch commercial system used for comparison.

An alternative strategy to improve capture efficiency by nanoneedles is to form branched hierarchical nanowires (ITO), instead of vertically oriented ones[15] (Figure 3C). Multi-step chemical vapor deposition can generate hierarchical nanowires where multiple generations of orthogonal branches stem from the initial vertical nanowire. Flat ITO surfaces capture EpCAM positive cells with 1.4% efficiency, while vertical ITO nanowires have a 67% efficiency. Adding one generation of branches increases efficiency to 85% and the second generation further enhances it to 89% while maintaining elevated cell viability. Embedding gold nanoclusters within the surface of the wire also improves capture efficiency[66]. With rapid thermal chemical vapor deposition, it is possible to simultaneously grow long nanowires (Si) and decorate their surface with gold nanoclusters, due to the rapid diffusion of the liquid Au Si on the Si substrate. At 5 minutes of incubation with cells system has a low capture yield of 4% for pure Si nanowires which increases to 40% with for annealed, Au coated nanowires. When increasing incubation to 40 minutes, the capture yields rise to ~40% and over 80% respectively. Thanks to the strong absorption of the Au nanoclusters in the NIR, it is possible to combine selective capture of CTCs with photothermal therapy inducing their death.

Polymer-based nanotubes can capture CTC with approximately 80% efficiency[21]. The nanotubes (PS) are made by molding within an anodized alumina template, followed by partial backetching of the template to expose them. The backetching controls the length of the nanotubes and in turn their stiffness. Longer, and less stiff nanotubes capture CTCs more efficiently. Non-specific adhesion of cells for this system is approximately 20%. Cells spiked within blood at concentrations from 2 to 250 ml^{-1} are captured with 60% efficiency.

Thermal-responsive polymers grafted on nanowires (Si) enable reversible capture of CTCs[30] (Figure 3D). The capture system consists of anti-EpCAM antibody linked through biotin-streptavidin to a poly(*N*-isopropylacrylamide) (PNIPAm) grown onto silicon nanowires by a surface initiated atom-transfer radical polymerization. In this system the capture antibody is exposed when the PNIPAm is coiled above its transition temperature (T_c), and becomes hidden when PNIPAm is extended below T_c. In general PNIPAm above T_c supports cell attachment while it induces their detachment below T_c, regardless of the presence of the capture antibody[67]. Leveraging this ability, the system can capture CTCs at densities as low as 10 cells ml^{-1} with >70% efficiency. For 1000 cells ml^{-1}, capture and release efficiency is over 90%, and over 90% of released cells are viable. By releasing viable cells, this system rapidly enables their downstream culturing, expansion and further analysis.

Otherwise, laser scanning cytometry (LSC) can directly integrate CTC analysis on the nanowire (SiO_2) capture device[65] (Figure 3E). LSC provides high content, high throughput quantitative analysis of cell function through large area fluorescence images of cells and their analysis with image quantitation algorithms. Suspensions of 200 to 2000 ml^{-1} CTCs spotted on nanoneedles arrays defined with PDMS microwells can be fluorescently stained and imaged in situ by LSC. The analysis can count cells down to numbers of 10-60 per well, providing accurate indication of the capture yield (65%) and extracting several physical parameters of the captured cells. When mixing CTCs with peripheral blood mononuclear cells (PBMC) or with human blood, the LSC approach can distinguish CTCs thanks to their larger size and detect them at extremely low concentrations. In the clinical environment though, the CTC population would be largely inhomogeneous. While LSC would represent a useful technique to extract information regarding the composition of the CTC population in the clinic, it would require a more advanced approach to discriminate them from other circulating cells.

Nanoneedle-based sensors significantly increase the capture efficiency compared to the same material without nanoformulation. They detect as little as 2 cells ml^{-1} or 15 cancer cells within 1 million blood cells. When compared head-to-head with commercially available solutions, nanoneedle systems detect more cells in more patients.

System	Highest capture efficiency (%)	Non-specific capture (%)	Lowest captured conc (cells ml^{-1})	Ref
Si NWs	65	N/A	5	64
Si NWs + microfluidic	>95	N/A	50	54
ITO multibranch nanowires	89	~10	N/A	15
Au nanoclusters within SiNWs	>80	N/A	N/A	66
Polystyrene nanotubes	80	20	2	21

PNIPAm coated Si NWs	>90	N/A	10	[30]
SiO_2 nanopillars	65	N/A	15	[67]

Table 2 Key characteristics of nanoneedle systems for circulating tumour cell detection.

Sensing Cell Forces

Regulating forces at the nanoscale level is an important mechanism for cell signaling with implications in growth, migration and development. Crucial cellular processes including adhesion, cell-cell contact, division and migration involve orchestrated variations of forces within the cell both as effectors and as signaling components. Cytoskeletal tension and its interplay with the extracellular matrix has a strong influence in determining the fate of pluripotent cells.[68,69] Locally sensing the forces applied by cells to their environment is a crucial component to improve our understanding of their role within these fundamental cellular processes. Indeeed, measuring the displacement caused by cell tension on silicone micropillars and microbeads dispersed within silicone layers have provided important insights over the forces involved in cellular processes such as migration and division[70]. Thanks to their high packing density, small size and wide range of stiffness, nanoneedles have a great potential to detect small forces with high spatial resolution.

Nanoimprinted polycarbonate pillars imaged by electron microscopy can detect cellular forces[71]. They highlight the difference in the arrangement of forces between round non-migrating cells display a symmetric traction force profile, and elliptical, migrating cells with an asymmetric profile, characterized by larger forces at the leading edge. The system can also map forces across single cells, highlighting larger traction forces at the periphery than at the center.

Nanowires (GaP) grown by epitaxy on electron-beam lithography defined gold nanodots can measure cellular forces as small as 15 piconewton[17] (Figure 4A). Plating cells mouse dorsal root ganglia explants on the nanowires allows following the forces generated at the growth cone during pathfinding. Imaging the tip of the nanowires by confocal microscopy at 1 to 10s intervals tracks their displacement from the rest location, and calculating the associated forces. The quality of the force estimation is improved by using stroboscopic imaging to experimentally measure the Young's modulus of the nanowires, rather than relying on theoretical estimates. With prolonged imaging, this strategy allows monitoring the changes in the direction of force application over time, which reflect the dynamics of the growth process of the leading edge of neural fibers. Following the displacement of multiple nanowires simultaneously over time, allows building a force map with nanoscale space resolution and sub-second time resolution. A typical array can monitor over 20,000 points in a 140x140 μm^2 with a resolution of with 1µm. By modulating the length and diameter of the wires it is possible to tailor the spring constant and measure forces across different ranges. With long and thin nanowires forces as small as 15pN are detectable. In comparison, optical tweezers measure forces down to a single pN[72], but only for a few points simultaneously.

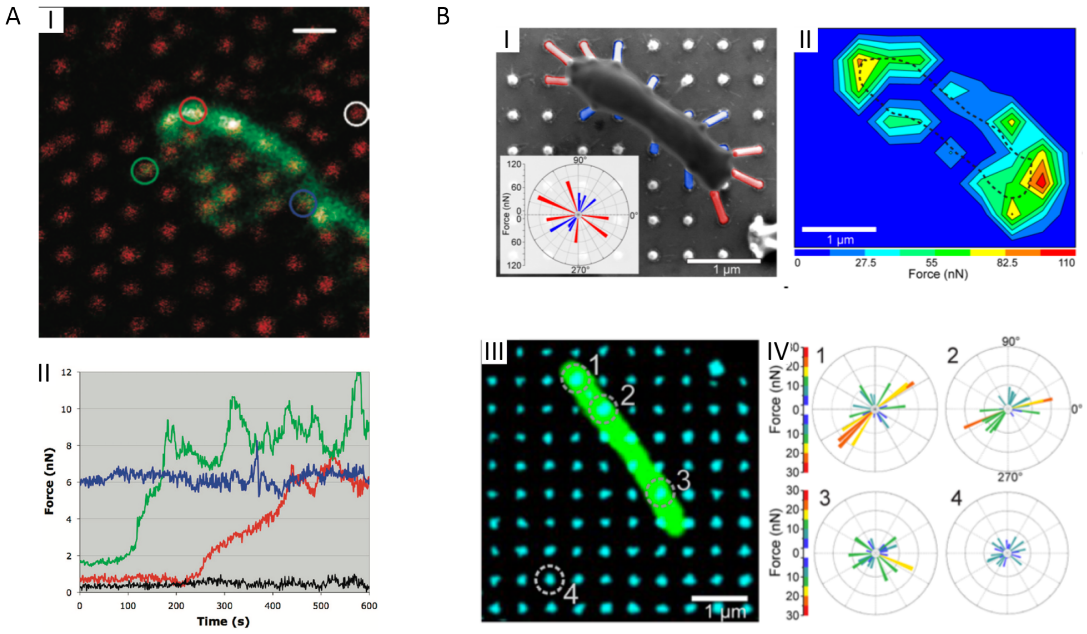

Figure 4 Sensing cell forces. The flexibility of nanoneedles and their trackability as single, point-wise isolated elements enables measuring forces exerted by cells on the substrate by evaluating the deflection of nanoneedles over time. (A) Confocal microscopy can track (I) the movement of single nanowires within an array during the extension of a growth cone. (II) Using the known mechanical properties of the nanoneedles it is possible to track the evolution of the force magnitude over time for each nanowire, potentially providing force tracking at sub-micron resolution, with 15 piconewton limit of detection. Reprinted with permission from [17]. Copyright 2010 American Chemical Society. (B) Scanning electron microscopy (I-II) and confocal microscopy (III-IV) can map the intensity and direction of the forces exerted by a bacterial cell on each nanoneedle within a large array. This approach can be extended to map forces across biofilm in culture and to detect the effects of surface coating on bacterial adhesion forces. Reprinted with permission from [73]. Copyright 2016 American Chemical Society.

Nanoneedles can also monitor the forces exerted on the substrate by individual bacterial cells and biofilms[73] (Figure 4B). Nanowire arrays (InP) with 500nm spacing can monitor the forces generated by *X. fastidiosa* seeded on them by electron microscopy or by confocal microscopy. This approach measures forces in the order of the tens of nN. Electron microscopy analysis shows that the poles of the bacteria exert larger forces than the cell bodies, although this measurement may suffer from sample processing artifacts. Optical microscopy imaging allows distinguishing the orientation of cells with respect to the substrate, and to build dynamic traction forces map for vertical and horizontal oriented cells. The role of adhesion molecules in modulating increasing the attachment of bacteria to surfaces, can also be monitored by coating the molecules over the nanowires and comparing the ensuing traction forces. Further, the mechanisms and strength of adhesion of bacterial biofilms can be tracked by this device. This analysis can provide valuable data when devising strategies to minimize bacterial adhesion and prevent biofilm formation and growth.

Electrical Sensing

Measuring intracellular electrical properties is greatly important to monitor the physiological state of excitable cells such as neurons and cardiomyocytes. Dysregulation of electrical activity in these cells, which often arises as the consequence of disorders in the regulation of

ion flow between cell compartments and across the cell membrane, cause pathological brain and heart dysfunctions that affect large portions of the population. Efficient and reliable sensing of intracellular electrical activity provides a platform to investigate the fundamental biology underlying such dysfunctions and to screen the therapeutic or detrimental effect of drugs.

Nanoneedles are ideally positioned as tools to measure intracellular potential for large populations of cells with minimal invasiveness. Unlike traditional intracellular electrophysiology probes, they can detect intracellular electrical signals without exchanging ions, thus minimizing the biochemical disturbance to cells. Further, their limited size reduces the insult to the cell membrane with respect to both micropipettes and microelectrode arrays, reducing associated toxicity and extending the duration of safe interfacing.

Single kinked nanowire field effect transistors (Si) can spatially probe local intracellular electrical activity[11]. They are operated with a micromanipulator and fuse with the cell membrane of rat neonatal cardiomyocytes when gently contacting it, thanks to a phospholipid coating. They can sense intracellular action potential within 1-20s following insertion due to membrane fusion, with a peak amplitude of 65mV and expected shape, consistent with simultaneous recording by patch clamping. The nanowire recording is stable for 5 minutes following insertion, longer than the 2.4 minutes achieved with patch clamping. Inserting two nanowires within adjacent cells allows monitoring intracellular action potential propagation across them. Similarly, single field effect transistors (bit-FET) can act as extracellular recorders of intracellular potential[45] (Figure 5A). They rely on a hollow nanotube gate (SiO_2) placed between a source-drain across a nanowire (Si). The nanotube extends orthogonally out of the substrates that hosts the nanowire. In this way the nanotube interfaces with cells as a nanoneedle. The variation in cytosolic potential are transferred within the nanotube, thus varying the potential of the gate electrode.

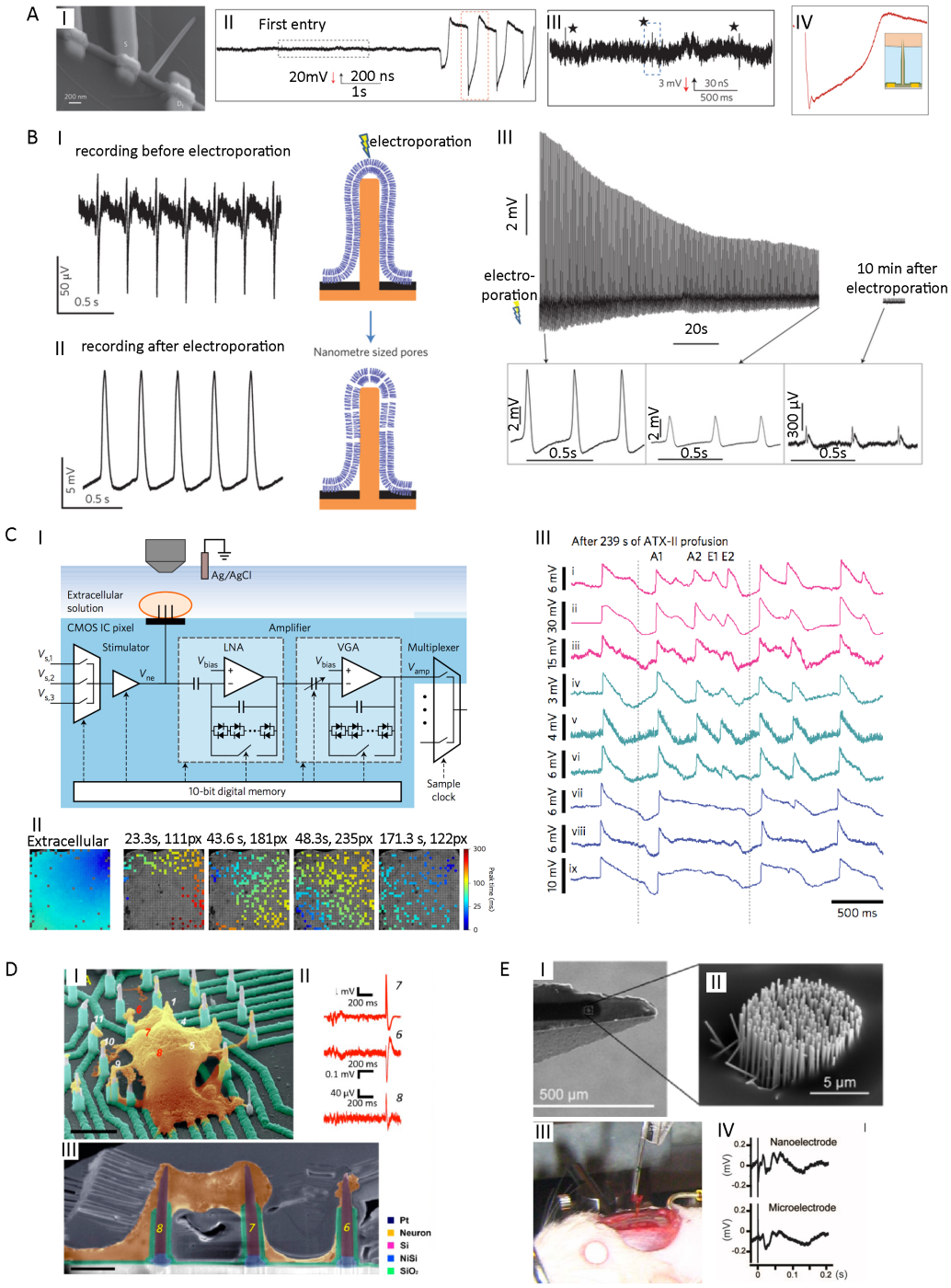

Figure 5 Electrical sensing. nanoneedles can access the intracellular fluid and record intracellular subthreshold and action potential electrical activity. (A) A field effect transistor (I) uses a nanotube as floating gate and functionalized with a phospholipid layer to fuse with the cell membrane (II) can be inserted within cells and measure intracellular action potentials. Magnification of the (III) extracellular and (IV) intracellular measurements within the black and red boxes of (II) respectively. *Scale bar 2 µm. Reprinted by permission from Macmillan Publishers Ltd: Nat. Nanotechnol.* [45]*, copyright (2012).* (B) Arrays of platinum nanopillars (I) record electrical activity extracellularly. They can deliver a train of voltage pulses to electroporate cells and (II) measure intracellular action potentials. (III) The

intracellular interfacing is progressively lost over the course of a few minutes. Reproduced with permission from *Reprinted by permission from Macmillan Publishers Ltd: Nat. Nanotechnol.* [32]*, copyright (2012)*. (C) An array of 1024 (32x32) independent nanoneedle electrical sensor arrays (I) can be packaged in a CMOS chip that integrates an amplifier to record electrical activity, a stimulator to deliver voltages and a memory to switch between the two for each pixel. Outside the array the circuit also integrates analog circuitry and multiplexers for near-simultaneous recording. (II) Almost all pixels within the array can couple extracellularly. Upon electroporation up to 235 pixels couple intracellularly and (III) monitor the propagation of action potentials across the cell culture. Intracellular access is time-dependent and is lost within few minutes. *Reprinted by permission from Macmillan Publishers Ltd: Nat. Nanotechnol.* [28]*, copyright (2017)*. (D) A high-density array of (I) independent nanoneedle electrodes can (II) record intracellular and extracellular electrical activity at multiple points within a cell. (III) SEM-FIB shows the cell-nanoneedle interfacing. *Reprinted with permission from* [74]*. Copyright 2017 American Chemical Society.* (E) A (I)spear electrode mounting an (II) array of nanowires can be (III) manipulated within the brain of a living animal to (IV) record potentials in agreement with those measured by standard microelectrodes. Reproduced under creative commons licence from[8].

The FET is particularly sensitive to potential variations (4,530 nS V) within the hollow core of the nanotube, and this in turn, due to its limited volume is highly sensitive to charge variation within the cell cytosol. The bit-FET has a temporal resolution better than 0.1ms, with an experimentally validated bandwidth of at least 6kHz. Phospholipid-modified bit-FETs placed in contact with a cell sheet can accurately record intracellular potential and can be re-used multiple times. Two bit-FTEs inserted within the same cardiomyocyte can simultaneously record action potentials propagating within it. Vertical nanoneedles supported on substrates can also measure intracellular potential. Small arrays (5 or 9) of metal nanoneedles acting as a single electrode can sense the intracellular action potential in cardiomyocytes and neurons cultured on them, in a setup similar to microelectrode arrays[6,32] (Figure 5B). The measurements require sending an initial train of voltage pulses of the order of few volts, in order to electroporate the cell and gain intracellular access. Once inserted, the nanoneedles can probe the intracellular action potential with a peak amplitude and shape that match simultaneous patch clamping records. The signal remains stable for few minutes, decaying to 30% of the initial value in just 120s in the case of cardiomyocytes[32]. With these recordings it is possible to distinguish between different specifications of cardiomyocytes (pacemaking and non-pacemaking) and neurons, and to assess the effects of drugs on the modulation of intracellular electrical activity.

These supported nanoneedle (Pt) electrodes can be scaled up to large arrays of independent electrodes[36]. These arrays can monitor the intracellular electrical activity of large number of cells within the same culture. Up to 60 cardiomyocytes simultaneously can be monitored in this way. This strategy also requires initial electroporation by the application of voltage pulses to initiate intracellular recording. The magnitude and waveform of the voltages recorded match very well those recorded by electroporation, and have a signal to noise ratio of 838 over a 5KHz bandwidth. This broad monitoring of multiple cells enables distinguishing subpopulations of ventricular-, atrial- and nodal-like cardiomyocytes within the larger cell population through the shape of their action potential. This system also tested human cardiomyocytes with different disorders. In hypertrophic cardiomyopathy cells it can reveal arrhythmia and delayed afterdepolarization. Importantly the system allows studying somatic cells differentiated from patient-derived human induced pluripotent stem cell (hIPSCs). The patient-derived hIPSC approach is an extremely promising strategy to investigate disease phenotypes and to screen candidate drugs[75,76]. Using the nanoneedles with HIPSCs derived

cardiomyocytes from long QT syndrome patients reveals the telltale action potential characteristics of the disease.

The nanoneedle electrode arrays (Pt/SiO_2) can be packaged within CMOS integrated circuits[28]. Each device contains an array of 1024 pixels (32x32) with a 126 μm pitch (Figure 5C). Each pixel includes the nanoneedle sensor array, composed of 9 nanocones with a SiO_2 core and a Pt conductive coating[6], connected to an amplifier to record electrical activity, a stimulator to deliver voltages and a memory to switch between the two. Outside of the array the IC also provides a control analog circuitry which includes multiplexers for nearly-simultaneous sampling at 9.75KHz. The system AC couples the amplifier to the nanoneedles and operates in double-layer capacitance mode. In this way the gain is flat across the band of electrophysiological recording and preserves the shape of the signal waveform. Further, this blocks DC current flow through nanoelectrodes, reducing the associated adverse effects to cell viability. Intracellular recording from the array requires initial electroporation by voltage pulse train and yields signals of the order of 5mV. This integration over a large number of cells enables network-level intracellular recording of cardiomyocyte cultures. Of the 1024 pixels, 968 are extracellularly coupled with cells enabling measuring the propagation speed of the action potential. Following electroporation 235 cells are intracellularly recorded. This setup measured over 250 beating cycles at a 5Hz frequency over the course of 50s. Typically more than 30% of the pixels couple intracellularly at some point, but over time the number fluctuates to a peak of 235 at 48s then reducing to 122 at 173s. This device can measure the difference in response to (drug) stimuli across a population of cardiomyocytes. When exposed to ATX-II, which mimics the effects of long-QT syndrome, the cells display a constant increase in action potential duration, but the device can identify that the degree of elongation varies with the different regions of the culture (Figure 5C III). The recording also reveals links between this inhomogeneity and the polarization dynamics across the network leading to arrhythmia within the cardiomyocyte sheet. The recording of these subthreshold membrane potential dynamics across a cellular network is unique to the nanoneedle array capacity to simultaneously monitor intracellular activty for a large number of cells, and cannot be achieved with patch clamps or microelectrode arrays.

At the opposite end of the integration spectrum, dense arrays of individually addressable nanoneedles (Si) can measure intracellular electrical activity with micron resolution[74] (Figure 5D). Silicon nanoneedles are lithographically defined and etched over pre-defined metallic pads, each interfacing with a single nanoneedle within an array of up to 60 elements, with a pitch of few microns. The needles can measure extracellular and intracellular action potential, with signals up to 100 mV. More importantly these devices can identify intracellular and extracellular electrical signals at subthreshold level, simultaneously in different regions of the cells. The device could measure intracellular subthreshold and action potentials from primary rat neurons for up to 14 days in culture and hIPSC derived neurons at six weeks in culture, indicating the potential for long-term monitoring of electrical activity in primary cultures.

Exploiting the hollow inner cavity of a 6x6 Iridium Oxide (IrOx) nanotubes array it is possible to prolong the duration of intracellular recording with nanoneedles[77]. In this setup the cell membrane invaginates within the cavity and, following electroporation, it establishes a more stable intracellular access. Further, sharing the hollow core structure approach of the bit-FET[45], this setup enhances cell-electrode coupling, yielding larger signals compared to solid nanoelectrodes. Compared to similar solid Au nanoneedles, the impedance of IrOx nanotubes is one order of magnitude lower, has a parallel resistor-capacitor behavior and has much lager

specific capacitance. With the IrOx nanotubes, following the initial electroporation, intracellular access is maintained for almost one hour, compared to the few minutes achieved with solid nanoneedles. The device allows monitoring the resealing of the membrane through a series of drops in signal amplitude over the course of several minutes, each of which last less than 2s. The poration can be repeated multiple times to monitor the action potential within the same cell over the course of eight consecutive days. This longitudinal recording shows an initial increase in recorded potential amplitude associated with cell maturation, followed by a decrease associated with ageing of the culture, demonstrating the potential for long term monitoring of intracellular electrical activity in culture systems.

Nanoneedles can move beyond cell cultures to measure electrical activity in more complex biological systems[58]. A single nanoneedle (W), operated through micromanipulators can record intracellular potential from neurons within brain slices. Hydrophobic silane functionalization, in principle similar to the phospholipid decoration[11], is necessary to achieve intracellular recording with this setup. The recordings last between 26 and 101 seconds, and it is possible to re-use the probe to re-interface with the target cell, in some instances. Both action potentials and subthreshold potentials can be recorder with this device. An array of nanoneedles (Au/GaP) can record electrical activity from the rat cerebral cortex *in vivo*[8] (Figure 5E). The array consists of nanowires with 500nm pitch over a circle with 12 µm diameter. The device substrate is cut so that the nanoneedle array resides on the side near the tip of a spear electrode that can be micromanipulated into the cortex of a living mouse. There, the nanoelectrode can record Aβ-fiber evoked field potential extracellularly. The potentials recorded well agrees with those recorded from a matched microelectrode. Further, the probe can record isolated single unit activity within the rat brain. The probe can be re-used multiple times, and the insertion-extraction process does not damage the nanoneedle array.

Sensing Biomolecules

Understanding the interplay processes that drive development, homeostasis and disease is the ultimate goal of systems biology. Similarly, the detection and measurement of concentration, localization, activity and interaction of biomolecules and ions in the intracellular and pericellular space with high spatiotemporal resolution and low limits of detection is crucial to advancing our understanding of biological interactions, and to improve the diagnosis and treatment of diseases. Nanoneedles interact with the intracellular space with minimal disturbance at the length scales at which molecular processes occur, and represent a unique tool to sense unperturbed biological systems with high resolution and sensitivity.

AFM operated single nanoneedles (Si) can monitor the intracellular environment[41]. Decorated with antibodies against specific proteins, they can be inserted within the cell, where they measure the antibody-ligand interaction by detecting steps in the force-displacement curve caused by unbinding events that occur during the retraction of the needle (Figure 6A). With this strategy it is possible to locally detect several cytoskeletal proteins, including actin[78], microtubules[31], nestin[79] and vimentin[41]. In all cases, non-specific interaction between the needle and intracellular molecules result in small force drops (~200 pN), while specific interaction with the target molecule generates larger and distinguishable drops in forces (>1 nN).

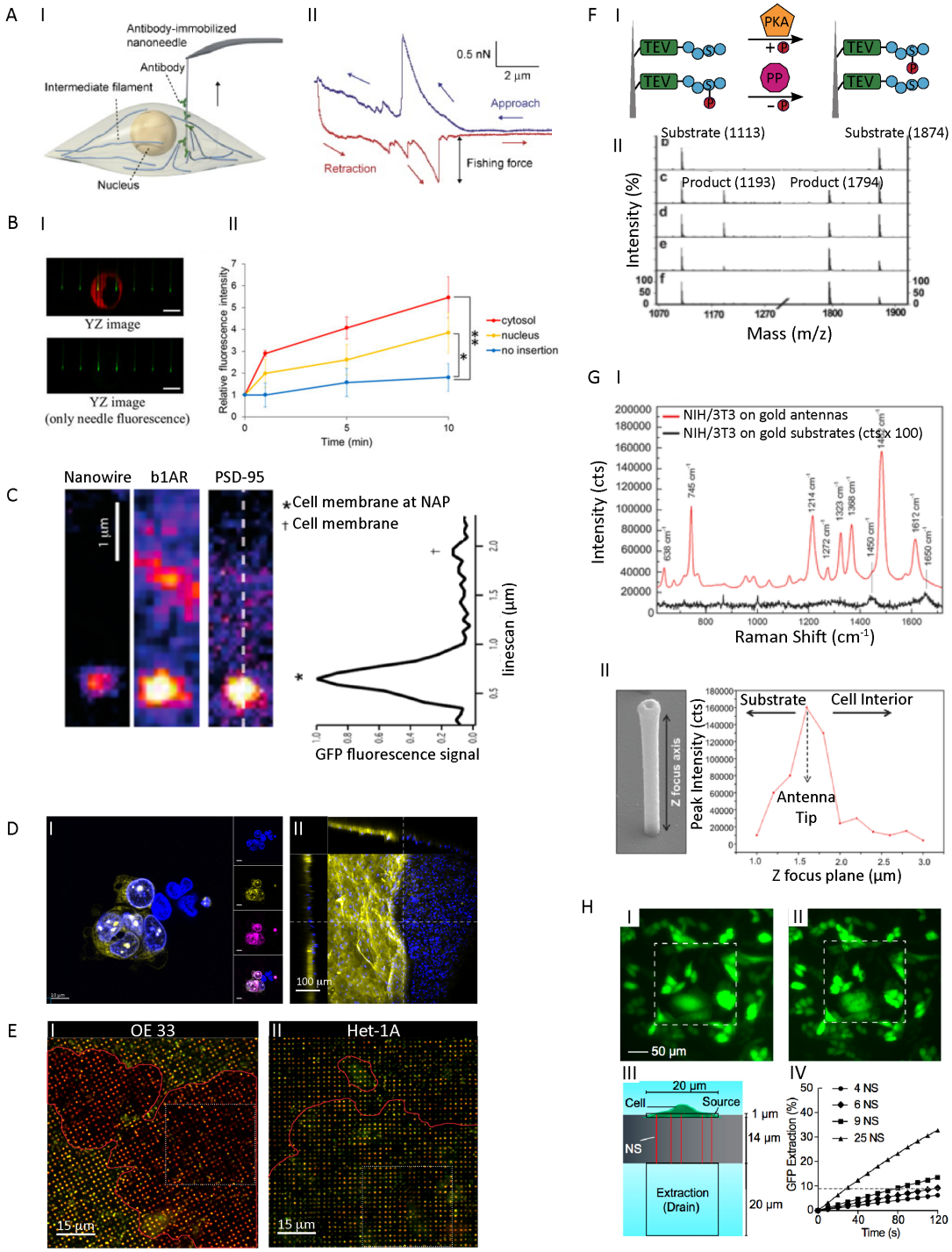

Figure 6 Sensing biomolecules. The access of nanoneedles to the intracellular milieu while inducing minimal perturbation provides a unique strategy to investigate intracellular biomolecules, their activity and their interaction. (A) AFM nanoneedles (I) decorated with antibodies can be inserted within cells to detect a specific target. (II) Upon retraction of the nanoneedles, drops in force of the order of 200pN and larger are associated with the unbinding of the antibodies from their ligand. Reprinted from [79], Copyright (2011), with permission from Elsevier. (B) Nanoneedles arrays (I) carrying a FRET molecular beacon (Green) interfaced with cells (Cytosol in red) can (II) detect intracellular GAPDH mRNA by a time-dependent change in FRET ratio. This strategy can discriminate the larger

mRNA concentration in the cytosol as opposed to the nucleus. Reproduced under creative commons licence from[61]. (C) The local enhancement of fluorescent signal due to the nanoneedle tip enables monitoring the interaction between b1AR and PSD-95 at the cell membrane by improving twenty-fold the co-localization signal with respect to what observed away from the nanoneedle tip. *Reprinted with permission from [47]. Copyright 2016 American Chemical Society*. (D) Nanoneedle arrays (I) functionalized with fluorescent Cathepsin B substrate peptides detect cells with high Cathepsin B cytosolic activity by highlighting their cytosol, in this way discriminating cancer cells from healthy ones through their metabolic activity. (II) This strategy applied to tissues can map intracellular Cathepsin B activity at the tumor margins, highlighting patches of high and low activity. Reproduced with permission from[18]. *Copyright © 2015 WILEY-VCH Verlag GmbH & Co. KGaA, Weinheim.* (E) Nanoneedle arrays functionalized with a pH sensitive dye (FITC) and a pH insensitive one (AF 633) maps intracellular and extracellular pH in cancer (OE33) and healthy (Het-1A) cells in culture, detecting the lower pH of cancer cells. *Reprinted with permission from [3]. Copyright 2015 American Chemical Society*. (F) Nanoneedle arrays (I) conjugated with peptide substrates for phosphatases and kinases can monitor the intracellular activity of these enzymes. (II) Mass spectrometry analysis of the peptides following cellular interfacing can monitor the addition and removal of phosphate groups over time as indicators of the intracellular activity of protein kinase A and PTP. *Reprinted with permission from[7]. Copyright 2013 American Chemical Society*. (G) Nanocone plasmonic antennas can identify the molecular composition of cells by SERS analysis(I). The SERS signal originating from the tip of an Ag/Au coated nanocone is $6.5x10^5$ higher than that obtained on flat plasmonic surfaces and allows detecting the signal from aromatic aminoacids, the secondary structure of membrane-associated proteins, cholesterol peaks, and the DNA backbone peak. (II) Moving away from the tip along the body of the nanoneedles, the enhancement rapidly vanishes. *Reprinted under creative commons license from[13]*. (H) Nanostraws can (I-III) extract intracellular fluid from cells and collect the biomolecules therein it for downstream analysis. (IV) The fraction of green fluorescent protein extracted can be monitored by optical microscopy and depends on the duration of the extraction and the number of extracting nanostraws. Reprinted with permission from[19].

This strategy allows monitoring both the number of drops occurring for each insertion and the intensity of the force, to provide a local understanding of the molecular composition. Optical probes attached to the AFM nanoneedle enable detecting protein activity and nucleic acids within cells by confocal microscopy. Conjugating a caspase-3 Förster Resonance Energy Transfer (FRET) probe to the AFM nanoneedle and inserting the nanoneedle within apoptotic cells allows monitoring caspase-3 activity through the changes in fluorescent signal[4]. This approach yields a 1.7-fold change in fluorescence upon exposure of the nanoneedle to an active Caspase-3 solution, and allows monitoring its activation within apoptotic HeLa cells. Despite the low Young's modulus of apoptotic HeLas (~10kPa) the needles insert with over 90% efficiency, and the decrease in FRET signal is detectable 60 minutes post insertion. Similarly, decorating the nanoneedle with a molecular beacon allows detecting GAPDH mRNA through the change in FRET signal upon insertion within the cell, although it only provides a modest signal increase preventing reliable quantifications[26]. Molecular beacons conjugated to arrays of diamond nanoneedles also monitor intracellular GAPDH mRNA expression levels, by quantifying the decrease in FRET signal over time following insertion[61] (Figure 6B). This strategy distinguishes the greater decrease in FRET signal for nanoneedles inserted within the cytosol from a smaller decrease associated with nuclear insertion, to provide spatially localized information. The fluidic force microscope (FluidFM) provides a 400nm nanochannel leading to a microfluidic reservoir integrated within a pyramidal AFM tip [80]. The FluidFM can approach and contact individual cells under optical microscopy guidance, and by applying underpressure, it can extract as little as 0.1pl of fluid from a single cell. The volume of the extracted fluid can be controlled with high precision. The FluidFM can specifically extract fluid

from either the nucleus or the cytosol, relying on optical guidance. This process is highly cytocompatible, with 82% of HeLa cells surviving the extraction of up to 4pl of cytosolic fluid and 86% of them surviving the extraction of up to 0.6pl of nuclear fluid. Instead the extraction of more than 4.5pl of cytosolic or 0.6pl of nuclear fluid invariably results in cell death. This is a striking result given that median cytosolic HeLa volume is estimated at 1.6 ± 0.7pl with a maximum of 4.4 pl, and their median nuclear volume is estimated at 0.7 pl. The extracts can be analyzed by electron microscopy to observe the ultrastructure of their vescicular and filamentous components. The enzymatic activity of β- galactosidase and Caspase 3 can be detected directly within the single-cell extract droplet. The FluidFM approach can also quantify the expression of genes and the relative localization of their mRNA in the nucleus and cytoplasm of a single cells by qPCR on the extract.

Single nanoneedles (SnO_2) operated through micromanipulators can act as intracellular endoscopes[20]. When mounted at the end of an optic fiber they can guide light within the cell to illuminate small intracellular volumes. Similarly, they can probe optical signals from subcellular regions at high spatial resolution. Using wires with high refractive index (n ~2.1-2.2) guarantees efficient light guidance within living cells (n ~ 1.3-1.5). The nanowire fiber can undergo multiple cycles of bending and bucking without damage. While bent its emission does not change significantly. The nanowire optical output is confined to its tip, providing a highly directional and localized illumination. The illumination of cells with blue light does not harm them thanks to the limited illumination volume. With the highly directional beam it is possible to illuminate quantum dots and intracellular fluorescent molecules locally, and visualize them by optical microscopy, while providing low background fluorescence for a high imaging contrast. The nanowire fiber can also couple incoming light originating from a cluster of QD in the cytosol. The intensity of light coupling is highly sensitive to the distance between the QD and the nanowire tip, providing a tool for high-spatial resolution mapping of fluorescent sources in three dimensions. The tip of these endoscopes (Si) can be functionalized with pH sensitive probes to detect local pH in small volume solutions, either by optical microscopy[35] or by Raman spectroscopy[35]. Optical measurements rely on pH sensitive ratiometric optical probes, while Raman sensing relies on SERS signals from pH-sensitive p-mercaptobenzoic acid. Photonic crystals, which can be extremely efficient biosensors[81], integrated on nanowire endoscopes (InGaAs) can insert within cells[33]. Their optical cavity consists of nanoholes within a GaAs structure hosting InAs QDs. Such cavity has a resonant mode at 1319nm with a Q factor of 1900. When inserted into cells the resonance shifts to 1345nm maintaining a Q factor of 2000. Cells well tolerate the insertion of the photonic probe for several days. As a model for its ability to detect biological interaction, a biotin-functionalized cavity allowed monitoring the binding of streptavidin in solution through a consistent redshift in its resonant mode.

Arrays of nanoneedles can also act as optical apertures, to limit the illumination or light acquisition regions, with the aim of locally improving signal to noise ratio and enhance signal detection. The high-aspect ratio geometry of nanoneedles (GaAs) generates photonic effects that modulates electromagnetic fields generating a “bright region”of enhanced field at the tip[47], and a “dark region” of suppressed field along the stem of the wire. This effect only occurs when nanowire-like structures are oriented vertically on their substrate. Further, the effect is more pronounced for shorter wavelengths, as the resonance peak is more tightly associated with the tip of the nanoneedles, while for wavelengths in the far red to infrared, the effect becomes negligible. When using these nanowires as waveguides with large

refractive index, the “bright region” decay provides a photon flux increase by a factor of 6, which decays exponentially from the tip with 45nm as characteristic length. The “dark region” along the nanowire stem can reach a diameter of 1.3 µm at the bottom of the nanowire. This generates an angular aperture of 55 degrees to the normal of the nanowires, where combining the incoming and outgoing photon enhancement with the waveguiding enhances fluorescent signals up to 20-fold, at 10nm from the tip. Using this setup, it’s possible to monitor molecular interaction, with a 12.8-fold specific signal enhancement over TIRF detection. This setup is ideally designed to investigate low-affinity interaction occurring at the cell membrane; indeed, the GaAs nanowires can detect the interaction between the G-protein-coupled receptor beta-1 adrenergic receptor and the intracellular scaffold protein postsynaptic density protein 95 (Figure 6C). The distance between the two proteins in the membrane is too large to monitor their interaction by FRET, but can be quantified in live cells by assessing co-localization. The presence of the nanoneedles enhances the fluorescent signal to background 20-fold compared to the off-needle signal within the same sample. Arrays of nanoscale apertures (SiO_2) can also be formed by transparent silicon dioxide nanopillars on a substrate coated with an opaque platinum layer[12]. The pillars generate an evanescent wave along their vertical surface that probes approximately 1 µm of the cell in the z-direction from the substrate. Single quantum dots can be attached to the tip of the pillars and excited through them to become switchable, point-like light sources. Thanks to the illumination mechanism, the light from these sources is detectable with a signal to background ratio of 5 within a solution containing 100nM of the same QDs. By coupling an anti-GFP antibody to the pillar is it possible to locally detect the fluorescence originating from GFP fused to a transmembrane protein, while eliminating the background signal that would otherwise arise from the cytosolic GFP.

Nanoneedle arrays can harvest and concentrate biomolecules from solution, in order to improve their detection. Specific harvesting of fluorescent streptavidin from solution on biotin-functionalized nanowires (InAs), and that of histidine tagged-GFP on Ni^{2+}:NTA nanowires (InAs) shows effective harvesting from solution and direct imaging on-needle without background, thanks to ability to image the tips and exclude background from non-specific adhesion to the substrate[23]. With this approach it is possible to calculate the streptavidin-biotin binding curve and estimate their binding affinity. The setup can also monitor a proof of principle of enzymatic activity by detecting the increase in fluorescence following the binding of SNAP-CLIP to its yellow fluorescent substrate BG-549. Similarly, nanowires (Si) decorated with antibodies for capture, can harvest a target protein from a spiked serum-like solution as well as real blood samples[22]. Its concentration can be monitored by fluorescence directly on the nanowires showing that over 90% of the spiked protein is collected on the nanowires. Concentrations as low as pM of proteins can be harvested and detected. By tuning pH and ionic strength the protein can then be then released from the substrate for use in downstream analysis. With this strategy, spiked cardiac troponin can be isolated and effectively filtered out from whole blood, and then released for electrical analysis in a nanowire-FET sensor downstream of the nanoneedle array.

Nanoneedles can also detect proteins and their interaction intracellularly. Nanoneedle arrays (C-diamond) functionalized with antibodies against NF-kB, can capture it intracellularly[34]. Once the nanoneedles are extracted from the cells, the protein is identified and quantified by immunofluorescence staining. This strategy allows monitoring the reduced cytoplasmic localization of NF-kB over time, following stimulation of interferon genes (STING). Similarly,

nanoneedle arrays (Si) can detect protein-interactions in a strategy similar to a pull-down assay [25]. Nanoneedles functionalized with anti c-abl antibody can specifically pull down the bcr-abl fusion protein from within a chronic myelogenous leukemia cell line. The fusion protein is then recognized with a sandwich immunofluorescence staining using an anti n-bcr antibody. With this strategy it is possible to monitor the interaction of Grb2 protein with the bcr-abl complex. The nanoneedle array with the sandwich immunofluorescence approach can simultaneously detect the presence of the fusion protein and its interaction with GrB2 by orthogonal immunofluorescence. The assay can also monitor the reduction of Grb2 interaction with brc-abl upon imantinib treatment. Similarly to the immunofluorescence strategy, the interaction can also be monitored by enzyme-linked immunoassay in an ELISA-like format.

Using fluorescently-labeled peptides as substrates, nanoneedles (Si) can detect the intracellular protease activity of Caspase-3[7] and Cathepsin B[2] (Figure 6D). In both cases the detection relies on the fluorophores that are retained within the cells' cytosol as a consequence of the cleavage of the peptide. Caspase-3 activity can be detected by sandwiching apoptotic cells between two nanoneedle arrays, one of which conjugated with a peptide substrate of Caspase-3. Following incubation, one of the array is removed and the accumulated fluorophore is observed. Cathepsin B detection instead uses a single nanoneedle array interfaced with cells cultured on a flat substrate[2]. This technique discriminates cancer cells from healthy ones within the same culture. Confocal microscopy or flowy cytometry analysis can detect at single cell level the the selective accumulation of fluorescent peptide fragments within the cytosol of cancer cells, due to their elevated Cathepsin B activity. Applying this strategy to biopsy samples of tumors can distinguishing normal and tumor regions and delineate intracellular Cathepsin B activity across tumor margin samples with resolution approaching that of single cells (Figure 6D). This same nanoneedle array (Si) can distinguish cancer cells from healthy ones by probing their intracellular pH[3]. Ratiometric measurement of the fluorescence intensity of a pH sensitive dye and a pH insensitive one simultaneously conjugated to the nanoneedles, maps pH across the array (figure 6E). The location of cancer cells with low pH can be detected in this way. The simultaneous delivery of a cell-impermeant payload during pH sensing and the lack apoptosis arising within these cells shows that sensing and delivery with nanoneedles are tightly interwoven processes, likely underpinned by common features of the unique nanoneedle biointerface, and that these interactions are well tolerated by cells.

Nanoneedle arrays (Si) with suitable peptide substrates can also monitor the activity of phosphatases and kinases using mass spectrometry analysis[7]. Nanoneedle arrays (Si) are efficient substrates for laser-assisted ionization in the absence of a matrix[82]. Particularly, silicon nanowires and nanopillars obtained by metal assisted chemical etching display a strong light adsorption that allows efficient desorption of ionized species upon laser irradiation. As with most matrix-free desorption strategies, desorption is most efficient in the low molecular range. Peptides and small molecules desorb from these substrates efficiently, enabling their detection with a performance comparable to regular MALDI approaches, but without the interfering signal from the matrix. Parameters such as the length of the needles, their spacing, their porosity, and their surface tension have strong effect on the performance of the substrate[83,84]. With this approach, nanoneedle arrays can detect the presence and concentration of illicit drugs in body fluid samples with a limit of detection as low as 32 ng/ml [84]. With the sandwich assay approach[7], it is possible to detect the addition and removal of

phosphate groups from the peptides immobilized to the nanoneedles by mass spectrometry. In this fashion the activity of protein tyrosine phosphatases and of protein kinase A (PKA) are monitored by observing the appearance of peaks corresponding to dephosphorylated and phosphorylated substrates respectively (Figure 6F) thus monitoring the kinetic of PKA following stimulation of cAMP.

Raman spectroscopy on nanoneedle arrays (Si/TiO_2) can detect biomolecules at the cell membrane. High density silicon nanowires have strong light adsorption across the UV-Visible and NIR spectrum, as a result of multiple, randomly oriented scattering events originating from the interaction with the electromagnetic radiation[85]. This property significantly increases the cross section for Raman scattering by increasing the scattering events, and simultaneously it suppresses Rayleigh scattering background. Superhydrophobic nanopillars arrays (Si) with a porous tip hosting Ag nanoparticles can concentrate molecules from solutions by localized droplet evaporation, while the porous structure fractionates small molecules against large abundant proteins, and the Ag nanoparticles enhance their Raman signal through SERS[86]. This setup can detect Rhodamine 6G at 10^{-12} M concentration in a background of albumin. Coating an array of nanoneedles with silver/gold bilayer provides a substrate with high plasmonic enhancement for SERS detection of cell membrane molecules[13]. When seeding cells on the array, the plasmonic hotspots come in close contact with cell membranes enhancing their Raman signal through SERS. The signal originating from the nanoneedles is 6.5 10^5 higher than that obtained on flat plasmonic surfaces (Figure 6G). In terms of pure field enhancement, this translates in the nanoneedles providing a 15-fold greater magnification of the incoming field than the flat plasmonic substrate. This enables detecting signal from aromatic aminoacids, the secondary structure of membrane-associated proteins, cholesterol peaks, and the DNA backbone peak. Moving away from the tip along the body of the nanoneedles, the enhancement rapidly vanishes in agreement with the observation about field modulation along these structures[46,47].

Thanks to their conduit to the intracellular space, arrays of nanostraws (Al_2O_3) can mediate repeated harvesting of intracellular fluid and/or delivery to the cell[19] (Figure 6H). Intracellular fluid containing proteins and nucleic acids can be harvested by applying an electroporation pulse. This method has >95% cell viability when repeated multiple times over the course of 20 days in astrocyte cultures derived from hiPSCs. The biomolecules can be concentrated and then analyzed by fluorescence, mRNA and ELISA detection strategies. Extraction from large cell populations is representative of the intracellular fluid composition as compared to lysates of the same cells, with reduced accuracy for large nucleic acids (> 16,000 nt). By detecting in real-time the loss of intracellular GFP fluorescence it is possible to establish that sampling occurs uniformly across the cell population. The loss of fluorescence indicates an extraction yield of approximately 6%, and suggests that 30% of the extracted protein is collected. Extraction from single cells is also possible, yielding between 7-8% of the intracellular protein amount, and reflects the composition of intracellular fluid, although the low amount of extracted materials limits analytical options. With this strategy it is possible to monitor the temporal changes in the expression of heat shock proteins upon cell stimulation, over the course of several days. The ability of nanostraws (Al_2O_3) to deliver payloads enables sensing of intracellular metabolic processes[27]. Nanostraws can deliver poorly membrane-permeable azido-functionalized monosaccharides into cells, where they undergo enzymatic processing that incorporates them within glycoproteins and traffics them to the cell membrane.

Orthogonal labeling of the saccharides at the membrane through the azido groups enables monitoring the metabolic processing that leads to their incorporation within glycoproteins.

Covalently immobilized 4-amino-1,8-naphthalic anhydride onto silicon nanoneedles, followed by the incorporation of the azide moiety within the fluorophore assembles a selective sensor for H_2S, which is the third endogenous gaseous transmitter in the human body[87]. This setup can detect H_2S by concentration-dependent changes in fluorescence intensity down to 7.1 mM, displaying potential for its quantitative analysis. The transmitter can be detected with high selectivity towards reactive sulfur, oxygen, and nitrogen species. Dissolved H_2S in cell culture media at physiological concentrations is detectable in the presence of cells.

Binding an aptamer to nanoneedles arrays (Si), these can sense the presence of ATP[88]. The ATP-binding aptamer releases the fluorescent label in solution in an ATP-dose and time-dependent manner at concentrations relevant for intracellular ATP detection. The aptamer is specific for ATP, since the addition of a comparable concentration of CTP does not induce a response. The decrease in fluorescence originating from ATP-sensing nanoneedles inserted within HeLa cells is more rapid and pronounced than that of neighboring nanoneedles not inserted within the cells, indicating that this approach can detect the higher intracellular ATP concentration.

Conclusions

The wide variety of nanoneedles systems available have demonstrated the flexibility to sense several key aspects of cell function with precision, at the nanoscale and with translational potential. The more advanced sensing of electrical activity is currently capable of fully integrated measurement of highly parallel signals with high throughput that highlights complex behaviors and their response to external stimuli with unprecedented precision. Sensing biomolecules, their interactions, and broadly intracellular conditions have the unprecedented ability to elucidate intracellular state of large number of cells with single-, or even sub-cell resolution and without significant perturbation. Nanoneedles can monitor the evolution of these conditions over time, and can sense within biological systems with widely varying degrees of complexity, all the way to biological fluids, tissues *ex vivo* and living organisms.

Yet, the wide range of systems and strategies used for sensing clearly highlights the fragmentation within the nanoneedle world, which stems from the widely different needs of each application, and translates in the inability to design a one-size-fits-all device. This fragmentation in turn hampers progress towards translation, as the portability of findings across systems is limited, and the discrepancies in observed phenomena that arise are not easily attributable to specific characteristics of the systems. As an added layer of complexity, each cell type and sensing modality represent an almost unique system, given the broad differences in cell morphology, size, mechanical properties and signaling networks involved. This, coupled with the very limited knowledge of the underlying principles of cell-nanoneedle interaction, requires an almost ex-novo optimization of nanoneedle systems for each cell/tissue target and for each intended sensing application. Further, despite the great and rapid advances, the vast majority of the literature proposes proof of principles, in largely idealized conditions, and their translation to the more complex and realistic systems is so far limited. The future success of nanoneedles for biosensing will crucially rely on the solutions provided to key challenges regarding a deeper understanding of the nature of the

biointerface, the translation of fundamental findings to complex, realistic systems and the combination of sensing principles into integrated designs and workflows.

ACKNOWLEDGEMENTS

Ciro Chiappini would like to acknowledge financial support from the Rosetrees Trust (A1501) and the Guy's and St. Thomas' Charity (R170503)

Vocabulary

Nanoneedle: A high aspect ratio nanostructure that interacts with the cell membrane and the intracellular environment. The definition comprises a broad range of nanomaterials including nanowires, nanopillars, nanocones, nanostraws and nanotubes. Nanoneedles come either as single elements operated by AFM/micromanipulators or as vertical arrays of nanostructures supported on substrates.

Biological system: A functional network of interrelated biologically relevant entities. Cells and their organelles are examples of nano- and micro-scale biological systems as their function has origin in the concerted action of biomolecules. Organs and organisms are example of macroscopic biological systems, as their function has origin in the concerted action of cells organized into tissues, organized into organs, organized into organ systems.

Biointerface: The region of contact between a biological system and an artificial one.

Biosensing: Sensing analytes of importance in the study of biological systems.

Invasiveness: The degree of unwanted perturbation induced on a biological system by interacting with it.

Intracellular electrical activity: The variation in intracellular ion concentrations tightly regulated through ion channels, that determines changes of potential across the cell membrane. These variations underpin the propagation of electrical signals in excitable cells.

Biomolecule: A molecule involved in the functioning of a biological system.

REFERENCES

(1) Shalek, A. K.; Gaublomme, J. T.; Wang, L.; Yosef, N.; Chevrier, N.; Andersen, M. S.; Robinson, J. T.; Pochet, N.; Neuberg, D.; Gertner, R. S.; *et al.* Nanowire-Mediated Delivery Enables Functional Interrogation of Primary Immune Cells: Application to the Analysis of Chronic Lymphocytic Leukemia. *Nano Lett.* **2012**, *12*, 6498–6504.

(2) Chiappini, C.; De Rosa, E.; Martinez, J. O.; Liu, X.; Steele, J.; Stevens, M. M.; Tasciotti, E. Biodegradable Silicon Nanoneedles Delivering Nucleic Acids Intracellularly Induce Localized in Vivo Neovascularization. *Nat. Mater.* **2015**, *14*, 532–539.

(3) Chiappini, C.; Martinez, J. O.; De Rosa, E.; Almeida, C. S.; Tasciotti, E.; Stevens, M. M. Biodegradable Nanoneedles for Localized Delivery of Nanoparticles in Vivo:Exploring the Biointerface. *ACS Nano* **2015**, *9*, 5500–5509.

(4) Kihara, T.; Nakamura, C.; Suzuki, M.; Han, S. W.; Fukazawa, K.; Ishihara, K.; Miyake, J. Development of a Method to Evaluate Caspase-3 Activity in a Single Cell Using a Nanoneedle and a Fluorescent Probe. *Biosens. Bioelectron.* **2009**, *25*, 22–27.

(5) Chiappini, C.; Liu, X.; Fakhoury, J. R.; Ferrari, M. Biodegradable Porous Silicon Barcode Nanowires with Defined Geometry. *Adv. Funct. Mater.* **2010**, *20*, 2231–

2239.
(6) Robinson, J. T.; Jorgolli, M.; Shalek, A. K.; Yoon, M.-H.; Gertner, R. S.; Park, H. Vertical Nanowire Electrode Arrays as a Scalable Platform for Intracellular Interfacing to Neuronal Circuits. *Nat. Nanotechnol.* **2012**, *7*, 180–184.
(7) Na, Y.-R.; Kim, S. Y.; Gaublomme, J. T.; Shalek, A. K.; Jorgolli, M.; Park, H.; Yang, E. G. Probing Enzymatic Activity Inside Living Cells Using a Nanowire–Cell "Sandwich" Assay. *Nano Lett.* **2013**, *13*, 153–158.
(8) Suyatin, D. B.; Wallman, L.; Thelin, J.; Prinz, C. N.; Jörntell, H.; Samuelson, L.; Montelius, L.; Schouenborg, J. Nanowire-Based Electrode for Acute in Vivo Neural Recordings in the Brain. *PLoS ONE* **2013**, *8*, e56673.
(9) Han, S. W.; Nakamura, C.; Obataya, I.; Nakamura, N.; Miyake, J. A Molecular Delivery System by Using AFM and Nanoneedle. *Biosens. Bioelectron.* **2005**, *20*, 2120–2125.
(10) McKnight, T. E.; Melechko, A. V.; Hensley, D. K.; Mann, D. G. J.; Griffin, G. D.; Simpson, M. L. Tracking Gene Expression After DNA Delivery Using Spatially Indexed Nanofiber Arrays. *Nano Lett.* **2004**, *4*, 1213–1219.
(11) Qing, Q.; Jiang, Z.; Xu, L.; Gao, R.; Mai, L.; Lieber, C. M. Free-Standing Kinked Nanowire Transistor Probes for Targeted Intracellular Recording in Three Dimensions. *Nat. Nanotechnol.* **2014**, *9*, 142–147.
(12) Xie, C.; Hanson, L.; Cui, Y.; Cui, B. Vertical Nanopillars for Highly Localized Fluorescence Imaging. *Proc. Natl. Acad. Sci. U.S.A.* **2011**, *108*, 3894–3899.
(13) La Rocca, R.; Messina, G. C.; Dipalo, M.; Shalabaeva, V.; De Angelis, F. Out-of-Plane Plasmonic Antennas for Raman Analysis in Living Cells. *Small* **2015**, *11*, 4632–4637.
(14) Peer, E.; Artzy-Schnirman, A.; Gepstein, L.; Sivan, U. Hollow Nanoneedle Array and Its Utilization for Repeated Administration of Biomolecules to the Same Cells. *ACS Nano* **2012**, *6*, 4940–4946.
(15) Zhang, F.; Jiang, Y.; Liu, X.; Meng, J.; Zhang, P.; Liu, H.; Yang, G.; Li, G.; Jiang, L.; Wan, L.-J.; *et al.* Hierarchical Nanowire Arrays as Three-Dimensional Fractal Nanobiointerfaces for High Efficient Capture of Cancer Cells. *Nano Lett.* **2016**, *16*, 766–772.
(16) Hanson, L.; Zhao, W.; Lou, H.-Y.; Lin, Z. C.; Lee, S. W.; Chowdary, P.; Cui, Y.; Cui, B. Vertical Nanopillars for in Situ Probing of Nuclear Mechanics in Adherent Cells. *Nat. Nanotechnol.* **2015**, *10*, 554–562.
(17) Hällström, W.; Lexholm, M.; Suyatin, D. B.; Hammarin, G.; Hessman, D.; Samuelson, L.; Montelius, L.; Kanje, M.; Prinz, C. N. Fifteen-Piconewton Force Detection From Neural Growth Cones Using Nanowire Arrays. *Nano Lett.* **2010**, *10*, 782–787.
(18) Chiappini, C.; Campagnolo, P.; Almeida, C. S.; Abbassi-Ghadi, N.; Chow, L. W.; Hanna, G. B.; Stevens, M. M. Mapping Local Cytosolic Enzymatic Activity in Human Esophageal Mucosa with Porous Silicon Nanoneedles. *Adv. Mater.* **2015**, *27*, 5147–5152.
(19) Cao, Y.; Hjort, M.; Chen, H.; Birey, F.; Leal-Ortiz, S. A.; Han, C. M.; Santiago, J. G.; Paşca, S. P.; Wu, J. C.; Melosh, N. A. Nondestructive Nanostraw Intracellular Sampling for Longitudinal Cell Monitoring. *Proc. Natl. Acad. Sci. U.S.A.* **2017**, *114*, E1866–E1874.
(20) Yan, R.; Park, J.-H.; Choi, Y.; Heo, C.-J.; Yang, S.-M.; Lee, L. P.; Yang, P. Nanowire-Based Single-Cell Endoscopy. *Nat. Nanotechnol.* **2012**, *7*, 191–196.
(21) Liu, X.; Chen, L.; Liu, H.; Yang, G.; Zhang, P.; Han, D.; Wang, S.; Jiang, L. Bio-Inspired

Soft Polystyrene Nanotube Substrate for Rapid and Highly Efficient Breast Cancer-Cell Capture. *NPG Asia Mater.* **2013**, *5*, e63.
(22) Krivitsky, V.; Hsiung, L.-C.; Lichtenstein, A.; Brudnik, B.; Kantaev, R.; Elnathan, R.; Pevzner, A.; Khatchtourints, A.; Patolsky, F. Si Nanowires Forest-Based on-Chip Biomolecular Filtering, Separation and Preconcentration Devices: Nanowires Do It All. *Nano Lett.* **2012**, *12*, 4748–4756.
(23) Rostgaard, K. R.; Frederiksen, R. S.; Liu, Y.-C. C.; Berthing, T.; Madsen, M. H.; Holm, J.; Nygård, J.; Martinez, K. L. Vertical Nanowire Arrays as a Versatile Platform for Protein Detection and Analysis. *Nanoscale* **2013**, *5*, 10226–10235.
(24) Zhang, A.; Lieber, C. M. Nano-Bioelectronics. *Chem. Rev.* **2016**, *116*, 215–257.
(25) Choi, S.; Kim, H.; Kim, S. Y.; Yang, E. G. Probing Protein Complexes Inside Living Cells Using a Silicon Nanowire-Based Pull-Down Assay. *Nanoscale* **2016**, *8*, 11380–11384.
(26) Kihara, T.; Yoshida, N.; Kitagawa, T.; Nakamura, C.; Nakamura, N.; Miyake, J. Development of a Novel Method to Detect Intrinsic mRNA in a Living Cell by Using a Molecular Beacon-Immobilized Nanoneedle. *Biosens. Bioelectron.* **2010**, *26*, 1449–1454.
(27) Xu, A. M.; Wang, D. S.; Shieh, P.; Cao, Y.; Melosh, N. A. Direct Intracellular Delivery of Cell-Impermeable Probes of Protein Glycosylation by Using Nanostraws. *ChemBioChem* **2017**, *18*, 623–628.
(28) Abbott, J.; Ye, T.; Qin, L.; Jorgolli, M.; Gertner, R. S.; Ham, D.; Park, H. CMOS Nanoelectrode Array for All-Electrical Intracellular Electrophysiological Imaging. *Nat. Nanotechnol.* **2017**, *110*, 609.
(29) Rivnay, J.; Wang, H.; Fenno, L.; Deisseroth, K.; Malliaras, G. G. Next-Generation Probes, Particles, and Proteins for Neural Interfacing. *Science Advances* **2017**, *3*, e1601649.
(30) Hou, S.; Zhao, H.; Zhao, L.; Shen, Q.; Wei, K. S.; Suh, D. Y.; Nakao, A.; Garcia, M. A.; Song, M.; Lee, T.; *et al.* Capture and Stimulated Release of Circulating Tumor Cells on Polymer-Grafted Silicon Nanostructures. *Adv. Mater.* **2013**, *25*, 1547–1551.
(31) Silberberg, Y. R.; Kawamura, R.; Ryu, S.; Fukazawa, K.; Ishihara, K.; Nakamura, C. Detection of Microtubules in Vivo Using Antibody-Immobilized Nanoneedles. *J. Biosci. Bioeng.* **2014**, *117*, 107–112.
(32) Xie, C.; Lin, Z.; Hanson, L.; Cui, Y.; Cui, B. Intracellular Recording of Action Potentials by Nanopillar Electroporation. *Nat. Nanotechnol.* **2012**, *7*, 185–190.
(33) Shambat, G.; Kothapalli, S.-R.; Provine, J.; Sarmiento, T.; Harris, J.; Gambhir, S. S.; Vučković, J. Single-Cell Photonic Nanocavity Probes. *Nano Lett.* **2013**, *13*, 4999–5005.
(34) Wang, Z.; Yang, Y.; Xu, Z.; Wang, Y.; Zhang, W.; Shi, P. Interrogation of Cellular Innate Immunity by Diamond-Nanoneedle-Assisted Intracellular Molecular Fishing. *Nano Lett.* **2015**, *15*, 7058–7063.
(35) Han, X.; Wang, H.; Ou, X.; Zhang, X. Silicon Nanowire-Based Surface-Enhanced Raman Spectroscopy Endoscope for Intracellular pH Detection. *ACS Appl. Mater. Interf.* **2013**, *5*, 5811–5814.
(36) Lin, Z. C.; McGuire, A. F.; Burridge, P. W.; Matsa, E.; Lou, H.-Y.; Wu, J. C.; Cui, B. Accurate Nanoelectrode Recording of Human Pluripotent Stem Cell-Derived Cardiomyocytes for Assaying Drugs and Modeling Disease. *Microsyst. Nanoeng.* **2017**, *3*, 16080.
(37) Berthing, T.; Bonde, S.; Rostgaard, K. R.; Madsen, M. H.; Sørensen, C. B.; Nygård, J.;

Martinez, K. L. Cell Membrane Conformation at Vertical Nanowire Array Interface Revealed by Fluorescence Imaging. *Nanotechnol.* **2012**, *23*, 415102.
(38) Hanson, L.; Lin, Z. C.; Xie, C.; Cui, Y.; Cui, B. Characterization of the Cell–Nanopillar Interface by Transmission Electron Microscopy. *Nano Lett.* **2012**, *12*, 5815–5820.
(39) Berthing, T.; Bonde, S.; Rostgaard, K. R.; Madsen, M. H.; Sørensen, C. B.; Nygård, J.; Martinez, K. L. Cell Membrane Conformation at Vertical Nanowire Array Interface Revealed by Fluorescence Imaging. *Nanotechnol.* **2012**, *23*, 415102.
(40) Xu, A. M.; Aalipour, A.; Leal-Ortiz, S.; Mekhdjian, A. H.; Xie, X.; Dunn, A. R.; Garner, C. C.; Melosh, N. A. Quantification of Nanowire Penetration Into Living Cells. *Nat. Comm.* **2014**, *5*, ncomms4613.
(41) Kawamura, R.; Shimizu, K.; Matsumoto, Y.; Yamagishi, A.; Silberberg, Y. R.; Iijima, M.; Kuroda, S.; Fukazawa, K.; Ishihara, K.; Nakamura, C. High Efficiency Penetration of Antibody-Immobilized Nanoneedle Thorough Plasma Membrane for in Situ Detection of Cytoskeletal Proteins in Living Cells. *J.Nanobiotechnol.* **2016**, *14*, 74.
(42) Han, S. W.; Nakamura, C.; Kotobuki, N.; Obataya, I.; Ohgushi, H.; Nagamune, T.; Miyake, J. High-Efficiency DNA Injection Into a Single Human Mesenchymal Stem Cell Using a Nanoneedle and Atomic Force Microscopy. *Nanomed. Nanotechnol. Biol. Med.* **2008**, *4*, 215–225.
(43) Singhal, R.; Orynbayeva, Z.; Kalyana Sundaram, R. V.; Niu, J. J.; Bhattacharyya, S.; Vitol, E. A.; Schrlau, M. G.; Papazoglou, E. S.; Friedman, G.; Gogotsi, Y. Multifunctional Carbon-Nanotube Cellular Endoscopes. *Nat. Nanotechnol.* **2010**, *6*, 57–64.
(44) Piret, G.; Perez, M.-T.; Prinz, C. N. Support of Neuronal Growth Over Glial Growth and Guidance of Optic Nerve Axons by Vertical Nanowire Arrays. *ACS Appl. Mater. Interf.* **2015**, *7*, 18944–18948.
(45) Duan, X.; Gao, R.; Xie, P.; Cohen-Karni, T.; Qing, Q.; Choe, H. S.; Tian, B.; Jiang, X.; Lieber, C. M. Intracellular Recordings of Action Potentials by an Extracellular Nanoscale Field-Effect Transistor. *Nat. Nanotechnol.* **2012**, *7*, 174–179.
(46) Frederiksen, R. S.; Alarcon-Llado, E.; Madsen, M. H.; Rostgaard, K. R.; Krogstrup, P.; Vosch, T.; Nygård, J.; Fontcuberta i Morral, A.; Martinez, K. L. Modulation of Fluorescence Signals From Biomolecules Along Nanowires Due to Interaction of Light with Oriented Nanostructures. *Nano Lett.* **2015**, *15*, 176–181.
(47) Frederiksen, R. S.; Alarcon-Llado, E.; Krogstrup, P.; Bojarskaite, L.; Buch-Månson, N.; Bolinsson, J.; Nygård, J.; Fontcuberta i Morral, A.; Martinez, K. L. Nanowire-Aperture Probe: Local Enhanced Fluorescence Detection for the Investigation of Live Cells at the Nanoscale. *ACS Photonics* **2016**, *3*, 1208–1216.
(48) Chiappini, C.; Martinez, J. O.; De Rosa, E.; Almeida, C. S.; Tasciotti, E.; Stevens, M. M. Correction to Biodegradable Nanoneedles for Localized Delivery of Nanoparticles in Vivo:Exploring the Biointerface. *ACS Nano* **2015**, *9*, 7730–7730.
(49) Elnathan, R.; Kwiat, M.; Patolsky, F.; Voelcker, N. H. Engineering Vertically Aligned Semiconductor Nanowire Arrays for Applications in the Life Sciences. *Nano Today* **2014**, *9*, 172–196.
(50) Xie, X.; Aalipour, A.; Gupta, S. V.; Melosh, N. A. Determining the Time Window for Dynamic Nanowire Cell Penetration Processes. *ACS Nano* **2015**, *9*, 11667–11677.
(51) Aalipour, A.; Xu, A. M.; Leal-Ortiz, S.; Garner, C. C.; Melosh, N. A. Plasma Membrane and Actin Cytoskeleton as Synergistic Barriers to Nanowire Cell Penetration. *Langmuir* **2014**, *30*, 12362–12367.

(52) Xie, X.; Xu, A.; Angle, M. R.; Tayebi, N.; Verma, P.; Melosh, N. A. Mechanical Model of Vertical Nanowire Cell Penetration. *Nano Lett.* **2013**, *13*, 6002–6008.
(53) Obataya, I.; Nakamura, C.; Han, S.; Nakamura, N.; Miyake, J. Mechanical Sensing of the Penetration of Various Nanoneedles Into a Living Cell Using Atomic Force Microscopy. *Biosens. Bioelectron.* **2005**, *20*, 1652–1655.
(54) Wang, S.; Liu, K.; Liu, J.; Yu, Z. T. F.; Xu, X.; Zhao, L.; Lee, T.; Lee, E. K.; Reiss, J.; Lee, Y. K.; *et al.* Highly Efficient Capture of Circulating Tumor Cells by Using Nanostructured Silicon Substrates with Integrated Chaotic Micromixers. *Angew. Chem. Int. Ed.* **2011**, *50*, 3084–3088.
(55) Han, S.; Nakamura, C.; Obataya, I.; Nakamura, N.; Miyake, J. Gene Expression Using an Ultrathin Needle Enabling Accurate Displacement and Low Invasiveness. *Biochem. Biophys. Res. Comm.* **2005**, *332*, 633–639.
(56) Almquist, B. D.; Melosh, N. A. Fusion of Biomimetic Stealth Probes Into Lipid Bilayer Cores. *Proc. Natl. Acad. Sci. U.S.A.* **2010**, *107*, 5815–5820.
(57) Almquist, B. D.; Melosh, N. A. Molecular Structure Influences the Stability of Membrane Penetrating Biointerfaces. *Nano Lett.* **2011**, *11*, 2066–2070.
(58) Angle, M. R.; Schaefer, A. T. Neuronal Recordings with Solid-Conductor Intracellular Nanoelectrodes (SCINEs). *PLoS ONE* **2012**, *7*, e43194.
(59) Lee, J.-H.; Zhang, A.; You, S. S.; Lieber, C. M. Spontaneous Internalization of Cell Penetrating Peptide-Modified Nanowires Into Primary Neurons. *Nano Lett.* **2016**, *16*, 1509–1513.
(60) Wang, Y.; Yang, Y.; Yan, L.; Kwok, S. Y.; Li, W.; Wang, Z.; Zhu, X.; Zhu, G.; Zhang, W.; Chen, X.; *et al.* Poking Cells for Efficient Vector-Free Intracellular Delivery. *Nat. Comm.* **2014**, *5*, 4466.
(61) Matsumoto, D.; Sathuluri, R. R.; Kato, Y.; Silberberg, Y. R.; Kawamura, R.; Iwata, F.; Kobayashi, T.; Nakamura, C. Oscillating High-Aspect-Ratio Monolithic Silicon Nanoneedle Array Enables Efficient Delivery of Functional Bio-Macromolecules Into Living Cells. *Sci. Rep.* **2015**, *5*, 15325.
(62) Yosef, N.; Shalek, A. K.; Gaublomme, J. T.; Jin, H.; Lee, Y.; Awasthi, A.; Wu, C.; Karwacz, K.; Xiao, S.; Jorgolli, M.; *et al.* Dynamic Regulatory Network Controlling TH17 Cell Differentiation. *Nature* **2013**, *496*, 461–468.
(63) Persson, H.; Købler, C.; Mølhave, K.; Samuelson, L.; Tegenfeldt, J. O.; Oredsson, S.; Prinz, C. N. Fibroblasts Cultured on Nanowires Exhibit Low Motility, Impaired Cell Division, and DNA Damage. *Small* **2013**, *9*, 4006–4016.
(64) Wang, S.; Wang, H.; Jiao, J.; Chen, K. J.; Owens, G. E.; Kamei, K. I.; Sun, J.; Sherman, D. J.; Behrenbruch, C. P.; Wu, H.; *et al.* Three-Dimensional Nanostructured Substrates Toward Efficient Capture of Circulating Tumor Cells. *Angew. Chem. Int. Ed.* **2009**, *48*, 8970–8973.
(65) Lee, S.-K.; Kim, G.-S.; Wu, Y.; Kim, D.-J.; Lu, Y.; Kwak, M.; Han, L.; Hyung, J.-H.; Seol, J.-K.; Sander, C.; *et al.* Nanowire Substrate-Based Laser Scanning Cytometry for Quantitation of Circulating Tumor Cells. *Nano Lett.* **2012**, *12*, 2697–2704.
(66) Park, G.-S.; Kwon, H.; Kwak, D. W.; Park, S. Y.; Kim, M.; Lee, J.-H.; Han, H.; Heo, S.; Li, X. S.; Lee, J. H.; *et al.* Full Surface Embedding of Gold Clusters on Silicon Nanowires for Efficient Capture and Photothermal Therapy of Circulating Tumor Cells. *Nano Lett.* **2012**, *12*, 1638–1642.
(67) Akiyama, Y.; Kikuchi, A.; Yamato, M.; Okano, T. Ultrathin Poly(N-Isopropylacrylamide) Grafted Layer on Polystyrene Surfaces for Cell

Adhesion/Detachment Control. *Langmuir* **2004**, *20*, 5506–5511.
(68) Donnelly, H.; Dalby, M. J.; Salmeron-Sanchez, M.; Sweeten, P. E. Current Approaches for Modulation of the Nanoscale Interface in the Regulation of Cell Behavior. *Nanomed. Nanotechnol. Biol. Med.* **2017**. doi:10.1016/j.nano.2017.03.020
(69) Lane, S. W.; Williams, D. A.; Watt, F. M. Modulating the Stem Cell Niche for Tissue Regeneration. *Nat. Biotechnol.* **2014**, *32*, 795–803.
(70) Roure, du, O.; Saez, A.; Buguin, A.; Austin, R. H.; Chavrier, P.; Silberzan, P.; Siberzan, P.; Ladoux, B. Force Mapping in Epithelial Cell Migration. *Proc. Natl. Acad. Sci. U.S.A.* **2005**, *102*, 2390–2395.
(71) Viela, F.; Granados, D.; Ayuso Sacido, A.; Rodríguez, I. Biomechanical Cell Regulation by High Aspect Ratio Nanoimprinted Pillars. *Adv. Funct. Mater.* **2016**, *26*, 5599–5609.
(72) Kuo, S. C.; Sheetz, M. P. Force of Single Kinesin Molecules Measured with Optical Tweezers. *Science* **1993**, *260*, 232–234.
(73) Sahoo, P. K.; Janissen, R.; Monteiro, M. P.; Cavalli, A.; Murillo, D. M.; Merfa, M. V.; Cesar, C. L.; Carvalho, H. F.; de Souza, A. A.; Bakkers, E. P. A. M.; *et al.* Nanowire Arrays as Cell Force Sensors to Investigate Adhesin-Enhanced Holdfast of Single Cell Bacteria and Biofilm Stability. *Nano Lett.* **2016**, *16*, 4656–4664.
(74) Liu, R.; Chen, R.; Elthakeb, A. T.; Lee, S. H.; Hinckley, S.; Khraiche, M. L.; Scott, J.; Pre, D.; Hwang, Y.; Tanaka, A.; *et al.* High Density Individually Addressable Nanowire Arrays Record Intracellular Activity From Primary Rodent and Human Stem Cell Derived Neurons. *Nano Lett.* **2017**, acs.nanolett.6b04752.
(75) Serio, A.; Bilican, B.; Barmada, S. J.; Ando, D. M.; Zhao, C.; Siller, R.; Burr, K.; Haghi, G.; Story, D.; Nishimura, A. L.; *et al.* Astrocyte Pathology and the Absence of Non-Cell Autonomy in an Induced Pluripotent Stem Cell Model of TDP-43 Proteinopathy. *Proc. Natl. Acad. Sci. U.S.A.* **2013**, *110*, 4697–4702.
(76) Barmada, S. J.; Serio, A.; Arjun, A.; Bilican, B.; Daub, A.; Ando, D. M.; Tsvetkov, A.; Pleiss, M.; Li, X.; Peisach, D.; *et al.* Autophagy Induction Enhances TDP43 Turnover and Survival in Neuronal ALS Models. *Nat. Chem. Biol.* **2014**, *10*, 677–685.
(77) Lin, Z. C.; Xie, C.; Osakada, Y.; Cui, Y.; Cui, B. Iridium Oxide Nanotube Electrodes for Sensitive and Prolonged Intracellular Measurement of Action Potentials. *Nat. Comm.* **2014**, *5*, 3206.
(78) Silberberg, Y. R.; Mieda, S.; Amemiya, Y.; Sato, T.; Kihara, T.; Nakamura, N.; Fukazawa, K.; Ishihara, K.; Miyake, J.; Nakamura, C. Evaluation of the Actin Cytoskeleton State Using an Antibody-Functionalized Nanoneedle and an AFM. *Biosens. Bioelectron.* **2013**, *40*, 3–9.
(79) Mieda, S.; Amemiya, Y.; Kihara, T.; Okada, T.; Sato, T.; Fukazawa, K.; Ishihara, K.; Nakamura, N.; Miyake, J.; Nakamura, C. Mechanical Force-Based Probing of Intracellular Proteins From Living Cells Using Antibody-Immobilized Nanoneedles. *Biosens. Bioelectron.* **2012**, *31*, 323–329.
(80) Guillaume-Gentil, O.; Grindberg, R. V.; Kooger, R.; Dorwling-Carter, L.; Martinez, V.; Ossola, D.; Pilhofer, M.; Zambelli, T.; Vorholt, J. A. Tunable Single-Cell Extraction for Molecular Analyses. *Cell* **2016**, *166*, 506–516.
(81) Lin, V. S. Y.; Motesharei, K.; Dancil, K.-P. S.; Sailor, M. J.; Ghadiri, M. R. A Porous Silicon-Based Optical Interferometric Biosensor. *Science* **1997**, *278*, 840–843.
(82) Wang, C.; Reed, J. M.; Ma, L.; Qiao, Y.; Luo, Y.; Zou, S.; Hickman, J. J.; Su, M. Biomimic Light Trapping Silicon Nanowire Arrays for Laser Desorption/Ionization of

Peptides. *J. Phys. Chem. C* **2012**, *116*, 15415–15420.
(83) Dupré, M.; Enjalbal, C.; Cantel, S.; Martinez, J.; Megouda, N.; Hadjersi, T.; Boukherroub, R.; Coffinier, Y. Investigation of Silicon-Based Nanostructure Morphology and Chemical Termination on Laser Desorption Ionization Mass Spectrometry Performance. *Anal. Chem.* **2012**, *84*, 10637–10644.
(84) Alhmoud, H. Z.; Guinan, T. M.; Elnathan, R.; Kobus, H.; Voelcker, N. H. Surface-Assisted Laser Desorption/Ionization Mass Spectrometry Using Ordered Silicon Nanopillar Arrays. *Analyst* **2014**, *139*, 5999–6009.
(85) Bontempi, N.; Salmistraro, M.; Ferroni, M.; Depero, L. E.; Alessandri, I. Probing the Spatial Extension of Light Trapping-Induced Enhanced Raman Scattering in High-Density Si Nanowire Arrays. *Nanotechnol.* **2014**, *25*, 465705.
(86) Gentile, F.; Coluccio, M. L.; Zaccaria, R. P.; Francardi, M.; Cojoc, G.; Perozziello, G.; Raimondo, R.; Candeloro, P.; Di Fabrizio, E. Selective on Site Separation and Detection of Molecules in Diluted Solutions with Super-Hydrophobic Clusters of Plasmonic Nanoparticles. *Nanoscale* **2014**, *6*, 8208–8225.
(87) Wang, H.; Mu, L.; She, G.; Shi, W. Silicon Nanowires-Based Fluorescent Sensor for in Situ Detection of Hydrogen Sulfide in Extracellular Environment. *RSC Advances* **2015**, *5*, 65905–65908.
(88) Matsumoto, D.; NISHIO, M.; Kato, Y.; YOSHIDA, W.; ABE, K.; Fukazawa, K.; Ishihara, K.; Iwata, F.; IKEBUKURO, K.; Nakamura, C. ATP-Mediated Release of a DNA-Binding Protein From a Silicon Nanoneedle Array. *Electrochem.* **2016**, *84*, 305–307.

For TOC only

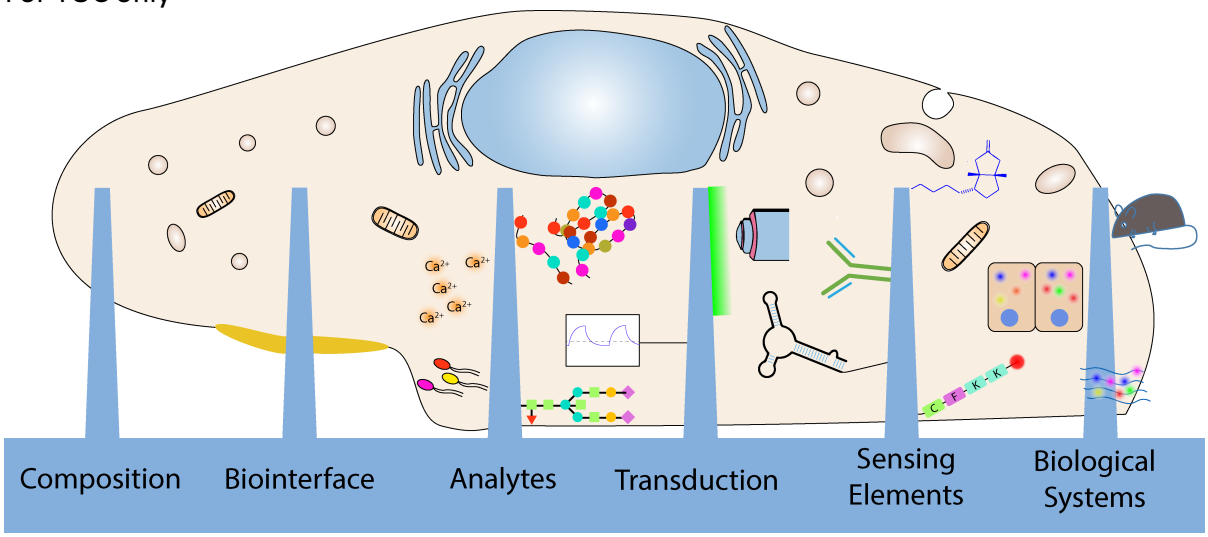
Composition
Biointerface
Analytes
Transduction
Sensing Elements
Biological Systems